

Whole Genome Association Study of the Plasma Metabolome Identifies Metabolites Linked to Cardiometabolic Disease in Black Individuals

Received: 15 September 2021

Accepted: 25 July 2022

Published online: 22 August 2022

 Check for updates

Usman A. Tahir^{1,185}, Daniel H. Katz^{1,185}, Julian Avila-Pachecho^{2,185}, Alexander G. Bick², Akhil Pampana², Jeremy M. Robbins¹, Zhi Yu², Zsu-Zsu Chen¹, Mark D. Benson¹, Daniel E. Cruz¹, Debby Ngo¹, Shuliang Deng¹, Xu Shi¹, Shuning Zheng¹, Aaron S. Eisman¹, Laurie Farrell¹, Michael E. Hall³, Adolfo Correa³, Russell P. Tracy⁴, Peter Durda⁴, Kent D. Taylor⁵, Yongmei Liu⁶, W. Craig Johnson⁷, Xiuqing Guo⁵, Jie Yao⁵, Yii-Der Ida Chen⁵, Ani W. Manichaikul^{8,9}, Frederick L. Ruberg¹⁰, William S. Blaner¹¹, Deepti Jain¹², NHLBI Trans-Omics for Precision Medicine 1 Consortium*, Claude Bouchard¹³, Mark A. Sarzynski¹⁴, Stephen S. Rich^{8,9}, Jerome I. Rotter⁵, Thomas J. Wang¹⁵, James G. Wilson¹, Clary B. Clish^{2,185}, Pradeep Natarajan^{2,16,185} & Robert E. Gerszten^{1,2,185} ✉

Integrating genetic information with metabolomics has provided new insights into genes affecting human metabolism. However, gene-metabolite integration has been primarily studied in individuals of European Ancestry, limiting the opportunity to leverage genomic diversity for discovery. In addition, these analyses have principally involved known metabolites, with the majority of the profiled peaks left unannotated. Here, we perform a whole genome association study of 2,291 metabolite peaks (known and unknown features) in 2,466 Black individuals from the Jackson Heart Study. We identify 519 locus-metabolite associations for 427 metabolite peaks and validate our findings in two multi-ethnic cohorts. A significant proportion of these associations are in ancestry specific alleles including findings in *APOE*, *TTR* and *CD36*. We leverage tandem mass spectrometry to annotate unknown metabolites, providing new insight into hereditary diseases including transthyretin amyloidosis and sickle cell disease. Our integrative omics approach leverages genomic diversity to provide novel insights into diverse cardiometabolic diseases.

Disturbed metabolism plays a central role across a spectrum of pathological processes from cancer to cardiometabolic disease^{1,2}. Metabolomics aims to systematically measure small molecules and provides a snapshot of metabolic activity, capturing both genetic and environmental influences on disease pathogenesis³. The integration of

genomics and metabolomics has been increasingly leveraged in efforts to identify bioactive metabolites linked to human disease, as large-scale genome-wide association studies (GWAS) have played a critical role in our understanding of loci that affect disease risk. Previous GWAS of the metabolome has identified associations between

A full list of affiliations appears at the end of the paper. ✉ e-mail: rgerszte@bidmc.harvard.edu

hundreds of genomic loci across a broad range of metabolite classes, including amino acids, nucleosides, and lipids among others^{4–24}. While prior studies have ranged in sample sizes from several hundred to a few thousand individuals, a recent study performed a GWAS meta-analysis across several large cohorts for 171 metabolites (in up to 86,507 individuals) measured using various metabolomic profiling platforms, including liquid chromatography-mass spectrometry (LC-MS) and nuclear magnetic resonance (NMR) spectroscopy²³. This cross-platform analysis highlighted the robustness of findings in metabolomics GWAS and the ability to detect clinically relevant associations, helping to illuminate biology in both common diseases such as diabetes and rare conditions such as macular telangiectasia type II.

Despite these efforts, the vast majority of metabolomics GWAS to date have been undertaken in cohorts of European ancestry, limiting the opportunity to leverage genomic diversity for biological discovery^{25–27}. Individuals of African ancestry are more genetically diverse than those of European ancestry²⁸, and carry ancestry-specific mutations which may illuminate biology and therapeutic strategies in cardiometabolic disease²⁹. Further, most GWAS of the metabolome to date have used genotyping arrays with measurement of a limited set of tag single nucleotide polymorphisms (SNP) with the imputation of remaining variants, limiting the ability to accurately assess low-frequency protein-coding and non-coding variation. Finally, while tools for unbiased metabolomic profiling can now measure hundreds of known metabolites as well as thousands of unknown metabolite peaks^{30,31}, the latter have eluded definitive compound identification, thus limiting biological insight into locus-metabolite associations. There are significant challenges in unknown metabolomic profiling, and attempts at further annotating these peaks in prior GWAS have been limited. First, unknown metabolite peaks must be separated from background noise and adduct ions of known and other unknown metabolites³². In addition, chemical identification of unique peaks requires downstream resource-intensive processes for structural elucidation, identification including the acquisition of product ion mass spectra (MS/MS) to generate metabolite fragmentation data as “chemical fingerprints” that can help improve compound identification³³. We have previously demonstrated proof-of-principle suggesting the utility of integrating LC-MS of unknown peaks with genetic findings.

For example, when peak levels map to solute carriers or enzymes with known functions, including substrates and products, this may help narrow the potential compound matches for chemical standard validation³⁴. However, this has remained an arduous process, limiting its application in metabolomics GWAS of unknown peaks in large population-based studies.

To extend prior work, we performed a genome-wide association study integrating whole genome sequencing (WGS) of 2,291 metabolite peaks in 2466 participants from the Jackson Heart Study (JHS), a Black epidemiological cohort in Jackson, Mississippi, and validated findings in the Multi-Ethnic Study of Atherosclerosis (MESA; $n = 995$) and Health, Risk Factors, Exercise Training and Genetics Family Study (HERITAGE; $n = 658$). Beyond confirming prior known locus-metabolite associations in a Black cohort—an important next step to test the generalizability of prior work—we highlight many novel findings, including associations in ancestry-specific alleles for heritable conditions more commonly observed in Black individuals, including transthyretin amyloidosis and sickle cell disease. We acquired MS/MS on metabolite features and have integrated WGS findings and recently developed bioinformatic tools that leverage MS fragmentation data for more efficient annotation and identification of unknown metabolite peaks. We have developed and made available an extensive sample library of metabolite peaks, linking MS/MS spectra, genomic associations, and clinical traits that can be leveraged for annotation and identification of unknown metabolites implicated in diverse disease processes. Our integrative omics approach highlights the value of whole genome sequencing analysis of the metabolome in diverse populations for biological discovery and contributes to a roadmap for the identification of metabolites implicated in human disease.

Results

We performed a whole genome association study (WGAS) in 2466 Black participants from JHS on 30,672,656 variants limited to an allele count of at least five against 2291 metabolites (337 known metabolites and 1954 unknown metabolites peaks; Fig. 1). Clinical characteristics of the study population are detailed in Supplementary Table 1. At a Bonferroni threshold of significance of $8E-11$ (based on $5E-8 / 602$

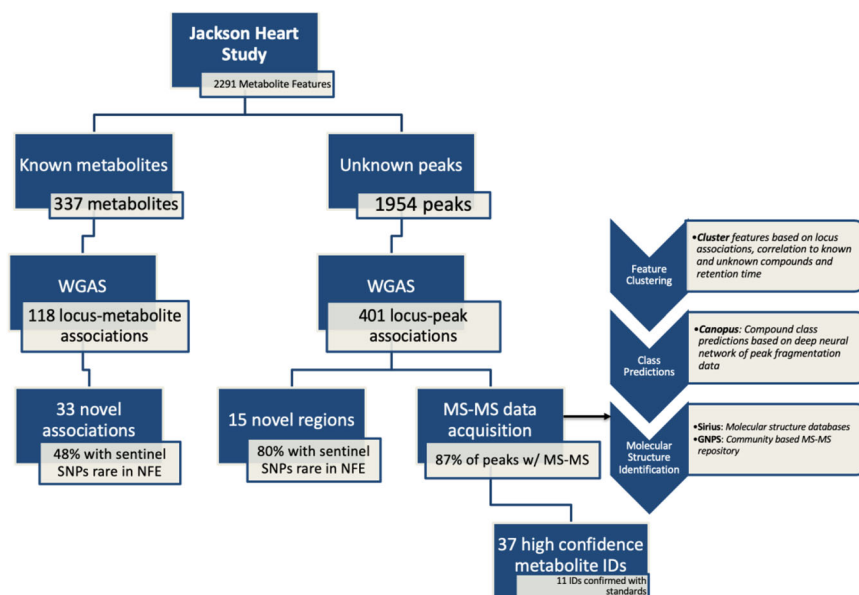


Fig. 1 | Whole Genome Association Study of known and unknown metabolites in the Jackson Heart Study. Flow diagram detailing whole genome association study of the metabolome, main results, and subsequent bioinformatic pipeline for unknown metabolite identification. Rare minor allele frequency is defined as $<1\%$ in

NFE using gnomAD. Confirmation of metabolite identities was limited to commercially available metabolite standards. WGAS whole genome association study, MS mass spectrometry; NFE non-Finish Europeans, GNPS global natural product social networking.

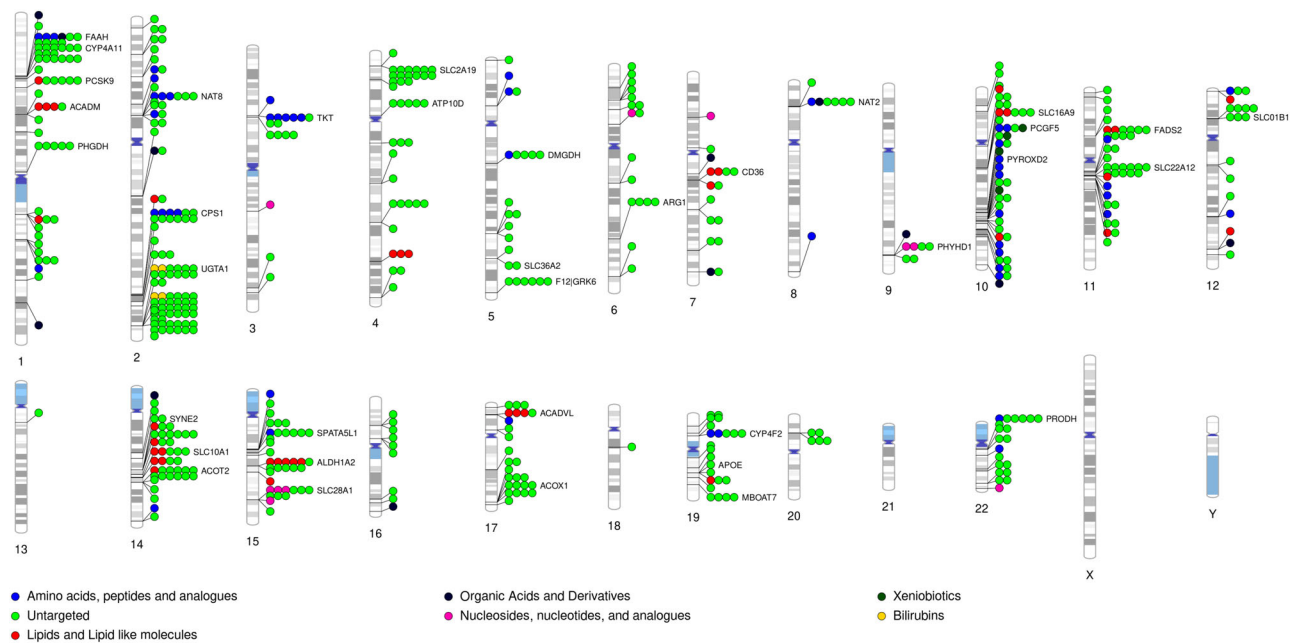


Fig. 2 | Phenogram of 519 locus-metabolite relationships in the Jackson Heart Study. 118 loci-metabolite associations are for known metabolites. 401 associations are for unknown metabolite features. The most common metabolite class includes

amino acids, peptides, and analogs. Highlighted are sentinel genes with ≥ 4 locus-metabolite associations.

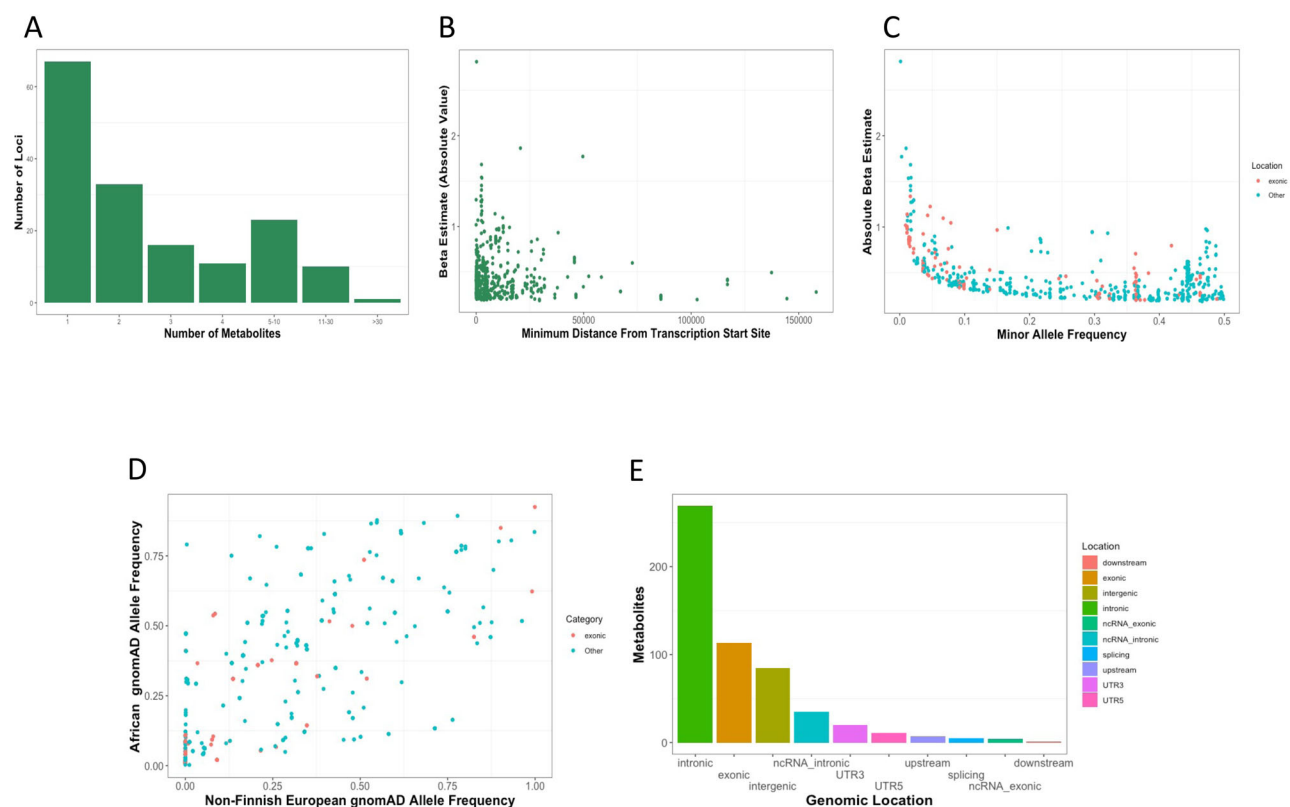


Fig. 3 | Genetic architecture of metabolite-WGAS associations. **A** Number of metabolites associated with each locus; **B** Absolute distance from mQTL position to transcription start site; **C** Minor allele frequency and effect size; **D** Frequency of

mQTL sentinel allele in non-Finnish European Individuals vs African individuals; **E** Location of mQTL. WGAS whole genome association study, mQTL metabolite quantitative loci.

principal components, which explain 95% of the variance in metabolite peak levels), there were 519 locus-metabolite associations, representing 427 metabolite peaks and 226 sentinel SNPs (Fig. 2). Of these, 118 locus-metabolite associations were determined from known metabolite analysis, representing 91 distinct metabolites. Comparison to prior GWAS of plasma metabolites, using publicly available summary statistics through PhenoScanner V2³⁵ and the GWAS Catalog³⁶ as well as manual review of previously published metabolomics GWAS (Supplementary Methods), suggests 33 of these locus-known metabolite associations are novel. In addition, we identified 401 locus-metabolite associations from the unknown metabolite peak analysis, representing 336 metabolite features, highlighting a large amount of information in the yet-to-be-identified peaks.

Of the 226 metabolite quantitative trait loci (mQTLs), there were 159 unique genes annotated as the lead candidate gene (closest protein-coding gene to the mQTL). Of the sentinel SNPs, 65% were expression quantitative loci (eQTL) for their corresponding gene as determined by PhenoScanner v2.0 (p value $<2E-4$; Supplementary Data 2). Of those that were not eQTLs for the candidate gene, the majority were rare in individuals of non-Finnish European Ancestry (MAF $<1\%$ in gnomAD), highlighting a key limitation of presently available genomic information when performing investigations in Black individuals. Among the sentinel SNPs, 22% were located in exons and an additional 19% were in enhancer or promoter regions (Fig. 3 and Supplementary Data 2).

Of the 519 locus-metabolite associations meeting the Bonferroni level of significance, 368 locus-metabolite peak relationships were available for validation in both MESA and HERITAGE, of which 91% were validated with a p value <0.05 and consistent direction of effect. An additional 100 locus-metabolite peak associations were available in either MESA or HERITAGE, of which 86% were validated. Overall, there was 90% validation of available locus-metabolite associations with p value <0.05 ; 68% validation (318 of 468 locus-metabolite associations available) using Bonferroni level of significance ($0.05/468$; p value $<1E-4$; Supplementary Data 2).

Ancestry-specific variants and metabolite associations

WGS of diverse populations provides an opportunity to assess allelic architectures of populations of different ancestries and inform underlying biology. In particular, for our study, 17% of the 226 sentinel SNPs that were rare (MAF $<1\%$) in Non-Finnish Europeans were common in individuals of African ancestry (MAF $>5\%$; Supplementary Data 2). Overall, 29% of the sentinel SNPs were nearly monoallelic in individuals of NFE ancestry with a MAF $<0.01\%$ in gnomAD³⁷. Here, we highlight several novel locus-metabolite relationships with SNPs that are rare in NFE (Table 1).

As an example, The *TTR* variant (V122I) is present in 3–4% of Black individuals and has been implicated in the pathophysiology of heart failure in the elderly, often unrecognized. We found the V122I in *TTR* to be associated with an unknown metabolite (m/z 269.226) in JHS ($\beta = -0.76$, p value = $4.4E-14$). The *TTR* tetramer complexes with retinol-binding protein (RBP4). This metabolite peak is correlated with RBP4 ($r^2 = 0.64$) measured by aptamer-based proteomic profiling³⁸ and V122I is significantly associated with RBP4 levels in JHS. Leveraging MS/MS data and its genetic association with *TTR* and correlation with RBP4, we predicted this compound to be all-*trans*-retinol (vitamin A), which we subsequently confirmed with an authentic standard (Supplementary Fig. 1). In addition, another variant that is nearly monoallelic in individuals of European ancestry, in *APOE* (rs769455), is associated with an unknown metabolite peak (m/z 269.226; $\beta = 0.71$, p value = $1.5E-12$) that has an identical molecular mass to all-*trans*-retinol (Fig. 4) and MS fragmentation analysis and MS comparison against chemical standards and all-*trans*-retinol and other retinol species predicts that it is a *cis*-isomer of retinol.

Annotation for unknown metabolite peaks associated with genomic loci

Of the 2291 metabolites measured, 1954 were unknown metabolite peaks, of which 336 were associated with genomic loci (p value $<8E-11$). Of the mQTLs associated with unknown features, 15 had no prior metabolite associations within 500 kb of the sentinel SNP; 12 of these SNPs were rare in individuals of NFE ancestry. (Supplementary Data 2). In the first step of assigning chemical identities to unknown metabolites, we clustered metabolite peaks measured in the positive mode (known and unknown metabolites) to identify primary metabolite features and their adducts (Supplementary Data 3). After applying our clustering algorithm, 49 of the 336 unknown metabolite peaks were part of clusters with known metabolites and were assigned the chemical identity of this primary metabolite. Of the 287 unknown metabolites not clustered with known compounds, 63 were adducts or fragments of other primary unknown metabolites, leaving 224 as major ions or primary unknown metabolites (Fig. 5).

Next, to aid in the identification of the unknown metabolites, we applied MS/MS profiling to metabolite peaks measured in positive mode, resulting in MS/MS data on 91% of unknown metabolite peaks designated as major ions or primary metabolites in our study. Using CANOPUS³⁹, a bioinformatics tool which uses MS/MS data to annotate chemical compound class for metabolites, 72% of primary unknown metabolite features were assigned a metabolite compound class; lipids, amino acids, and fatty acids were the most common metabolite groups. SIRIUS⁴⁰, a software tool that uses MS/MS data for metabolite structural elucidation, assigned chemical predictions in rank order for 182 primary unknown metabolites received (top three metabolite predictions for each feature in Supplementary Data 3). Leveraging these chemical predictions, we assigned high-confidence metabolite IDs to 33 metabolites that carried additional evidence for supporting the annotation using complementary tools, including Global Natural Product Social Molecular Networking (GNPS; $n = 8$)⁴¹, a database for MS/MS spectra in metabolomics studies, and the Human Metabolome Database (HMDB; $n = 5$)³², MS data for related compounds from our in-house metabolite library ($n = 12$) or validation with chemical standards ($n = 8$).

In addition to providing a database of MS/MS data for metabolomics studies, GNPS allows visualization of networks of structurally similar metabolites based on MS fragmentation data within studies to derive metabolite identities. As an example, chemical annotation using SIRIUS failed to generate a high-confidence metabolite prediction for an unknown metabolite with m/z 536.4354. However, using GNPS and comparing MS fragmentation data of this metabolite peak to community-based MS/MS spectra repositories, we were able to annotate this peak as carotene. Carotene is associated with rs2293440 ($\beta = 0.20$, p value = $4.73E-11$, an exonic variant in *Scavenger Receptor Class B Receptor 1 (SCARB1)*). SCARB1 plays a key role in lipoprotein metabolism through its action on reverse cholesterol transport and is associated with cholesterol levels in large population genomic studies⁴². Additionally, SCARB1 has been associated with the cellular uptake of carotenoids⁴³, increasing our confidence in our metabolite annotation. Using GNPS, we mapped structurally similar unknown metabolites based on MS/MS spectra (Fig. 6A). A closely related metabolite peak (m/z 568.427) with a cosine similarity score for fragmentation spectra of 0.88 (Fig. 6B; high similarity score designated as >0.7) was noted to be associated with the *Beta-carotene 15,15-dioxygenase (BCO1)* and *Intestine Specific Homeobox (ISX)* loci. BCO1 converts carotenoids to retinal and ISX participates in carotenoid metabolism by regulating the expression of BCO1⁴⁴. Anchoring our potential metabolite identification on these genomic associations, we searched through related carotenoid species based on mass differences between this peak and carotene and annotated this compound to be a carotenoid, zeaxanthin (Fig. 6D), which we subsequently validated with a chemical standard. In addition, the GNPS network identified

Table 1 | Ancestry-specific mQTLs in the Jackson Heart Study

rsID	Position	Metabolite	Gene	Position	Allele	Beta	P Value	AFR AF
rs141239670	Chr1:171219209	Succinic acid	SDHA	Exon	T	1.01	4.4E-11	0.01
rs56072071	Chr2:215328065	AICA-riboside**	ATIC	Intron	A	0.38	2.9E-17	0.11
rs754490766	Chr3:51959148	N-acetylglutamic Acid	PCBP4	Intron	A	1.40	3.0E-36	0.015
rs754490766	Chr3:51959148	N-acetylserine	PCBP4	Intron	A	1.06	1.2E-21	0.015
rs73733867	Chr6:44207081	N4-acetylcytidine	MYMX	Intergenic	T	1.29	1.9E-37	0.02
rs3211938	Chr7:80671133	C38:6 PE plasmalogen	CD36	Exon	G	0.38	1.6E-15	0.09
rs3211938	Chr7:80671133	C38:7 PC plasmalogen	CD36	Exon	G	0.38	1.6E-15	0.09
rs115027210	Chr7:76062732	2-Hydroxyglutaric Acid	MDH2	Exon	C	0.53	4.6E-16	0.05
rs28832309	Chr7:80690622	C40:7 PE plasmalogen	SEMACE3C	Intergenic	C	0.35	2.3E-12	0.09
rs7079286	Chr10:106656814	N(6),N(6)-dimethyl-lysine	F8MD8	Exon	T	-0.48	1.2E-23	0.11
rs334	Chr11:5227002	LPC(OH-16:0)*	HBB	Exon	A	0.48	4.19E-11	0.04
rs624307	Chr11:65376604	3-Hydroxycarnitine	SLC25A45	Exon	T	-0.42	7.6E-14	0.08
rs12322356	Chr12:56378580	UDP-GlcNAc	APOF	Intergenic	C	0.29	6.0E-17	0.31
rs13333418	Chr16:30975943	Cholestanone**	SETD1A	Exon	C	-0.23	1.4E-13	0.30
rs28934585	Chr17:7220519	CAR 14:1	ACADVL	Exon	T	-0.37	3.0E-15	0.11
rs28934585	Chr17:7220519	CAR 14:2	ACADVL	Exon	T	-0.38	1.8E-14	0.11
rs28934585	Chr17:7220519	CAR 12:0	ACADVL	Exon	T	-0.35	2.5E-13	0.11
rs76992529	Chr18:31598655	All-trans retinol**	TTR	Exon	A	-0.76	4.6E-14	0.02
rs12721054	Chr19:44919330	DG (36:4)	APOC1	UTR	G	-0.31	1.3E-11	0.12

Novel, ancestry-specific mQTLs for known and unknown metabolites in the Jackson Heart Study (minor allele frequency for sentinel SNP less than 1% in non-Finish Europeans).

AFR African, AF allele frequency, UTR untranslated region.

*Unknown metabolite annotated using MS/MS data.

**Unknown metabolite annotated with MS/MS and confirmed with the chemical standard.

another closely related compound in this network of unknown peaks, cryptoxanthin, a naturally occurring carotenoid compound.

Of the 37 high-confidence metabolite IDs from unique primary unknown metabolites (33 from SIRIUS predictions with supporting sources of information and four using GNPS; Supplementary Data 6), 92% (34/37) were evaluated as having genomic evidence in support of the chemical compound predictions based on the known metabolic pathways of the assigned lead candidate gene (Supplementary Data 2). In addition, CANOPUS annotated 29 of the 37 with metabolite class, of which 27 were in support of the metabolite annotation. We confirmed 11 unknown metabolite compound annotations with commercially available chemical standards; five of these are part of novel associations in a metabolomics GWAS: all-*trans*-retinol, zeaxanthin, 5,6 dihydrouridine, AICA-Riboside, and cholestanone (Supplementary Data 3 and Supplementary Fig. 1). MS/MS data on all metabolites associated with genomic loci in our study are made available (Supplementary Data 7).

Discussion

In the present study, we used WGAS to identify genetic determinants of plasma metabolites in a Black population from JHS and applied novel chemical profiling and bioinformatic methods to annotate unknown metabolite peaks. In our cohort of Black individuals, the presence of ancestry-specific alleles that are nearly monoallelic in individuals of European ancestry increases the power to detect novel metabolomic associations with established cardiovascular risk loci—and represents an important first step in the broader discovery of ancestry-specific, pathogenically significant metabolic differences.

In this study, we show a novel association in a clinically relevant polymorphism in *TTR* (*Transthyretin*), which is associated with increased risk of heart failure in Black individuals, and an unknown metabolite feature we identify as all-*trans*-retinol. The *TTR* V122I polymorphism described in 3–4% of Black individuals destabilizes the TTR-RBP4 tetramer, thereby displacing RBP4 and promoting amyloid fibril formation that precipitates heart failure and death⁴⁵. The reduced circulating all-*trans* retinol observed in our study may similarly be

related to increased clearance and a potential marker of TTR-RBP4 tetramer stability, as has been postulated in cases with ATTRv V122I amyloidosis⁴⁵. The effect of reduced all-*trans* retinol on downstream active retinol metabolites, including retinoic acid, and its potential contribution toward pathologic cardiac hypertrophy needs further study.

The *Apolipoprotein E* locus is a complex genomic region encoding APOE and the isoforms produced from its polymorphic alleles. APOE is involved in critical metabolic pathways, including lipid transport and metabolism⁴⁶, and is associated with chronic diseases, including the development of atherosclerosis and Alzheimer's disease, presumably mediated by its role in the transport and clearance of cholesterol and amyloid peptides to the brain⁴⁷. We show an association between a missense variant in *APOE* (rs769455), a nearly monoallelic polymorphism in individuals of European ancestry, with an unknown metabolite peak (*m/z* 269.226). This unknown metabolite has an identical molecular mass to all-*trans*-retinol and MS fragmentation analysis suggests that it is a potential isomer of retinol. While retinyl esters form with chylomicrons transported by APOE, the role of APOE transport on retinol species and potential downstream implications for retinoid transport and bioavailability has yet-to-be elucidated. Variants near retinoic acid transporters and receptors (downstream and active metabolites of retinol) have shown associations with risk for Alzheimer's disease and defective transport of retinol and related species has been implicated in this disease^{48,49}. Our findings showing associations between *APOE* and *cis*-retinol may have potential implications for the biological roles of APOE in disease pathways.

We show a novel association between an ancestry-specific variant in *CD36* (*Platelet Glycoprotein IV*; rs3211938) associated with specific plasmalogens, a subclass of phospholipids integral to cell membrane signaling and stability. CD36 is an integral transmembrane protein involved in the sequestration of malarial species, *plasmodium falciparum*, preventing splenic destruction of the organisms. As such, variants in *CD36* offer protection against malaria infection⁵⁰. In addition, CD36 functions as a receptor for several important inflammatory mediators, fatty acids, and lipids among others, and is implicated in

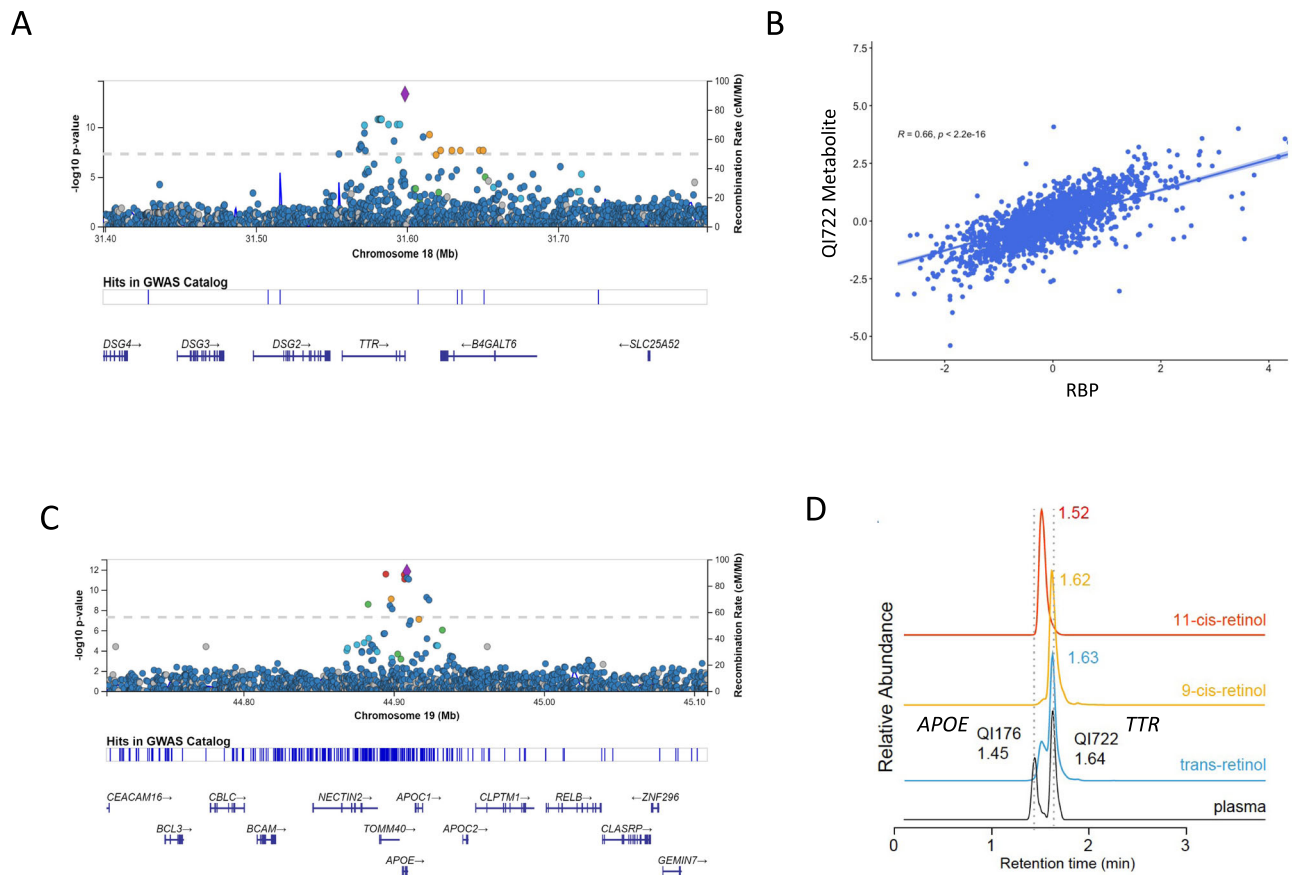


Fig. 4 | Ancestry-specific alleles reveal novel associations of TTR and APOE with retinol species. **A** Association of V122I in *TTR* with an unknown metabolite (QI722; *m/z* 269.226); **B** Correlation between QI722 and retinol-binding protein; **C** Association of rs769455 missense variant in *APOE* with unknown metabolite (QI176; *m/z* 269.226); **D** *TTR* associated unknown metabolite matching spectra with trans-retinol; *APOE* associated unknown metabolite with identical molecular mass but earlier retention time indicating it's a *cis*-isomer of retinol. Additional isomers tested without compound match include 9 and 11-*cis* retinol.

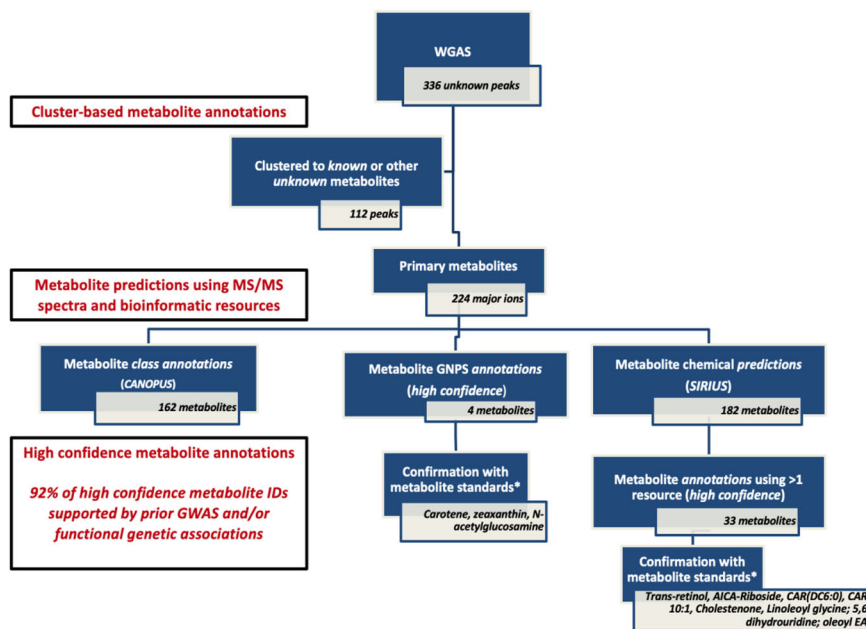


Fig. 5 | Unknown metabolite annotation pipeline using bioinformatic tools leveraging MS/MS spectra. Unknown metabolite identification with initial clustering of features to elucidate adducts and fragments of primary features or major ions. Subsequent implementation of tools leveraging MS/MS data, including SIRIUS, GNPS, and CANOPUS. Metabolite ID validation is limited to commercially available standards.

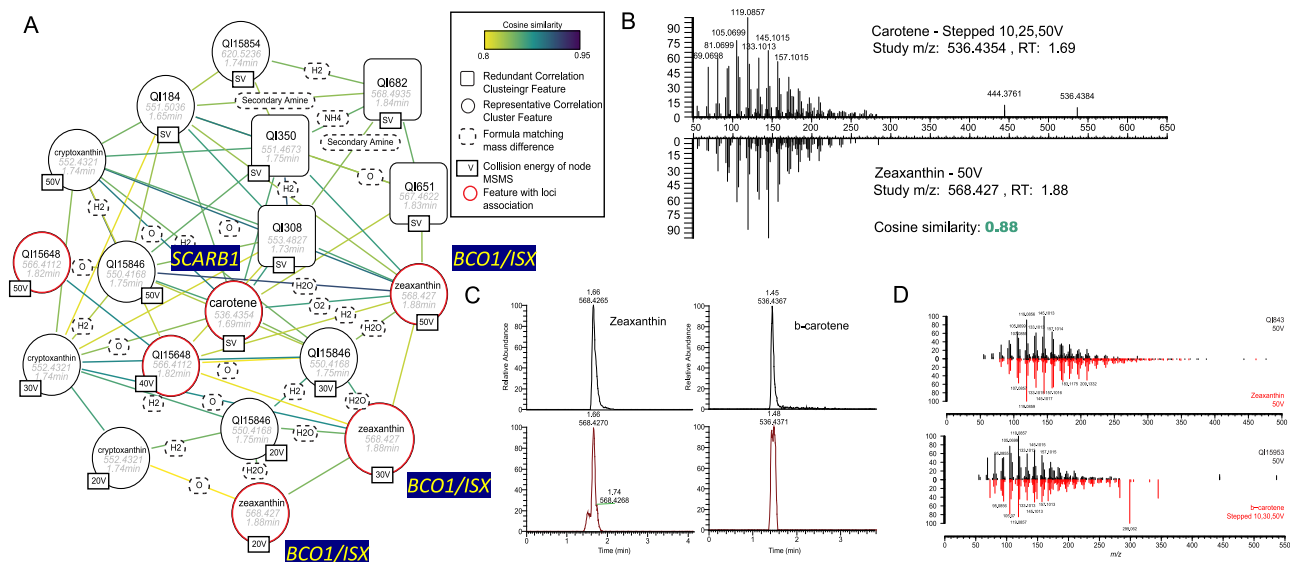


Fig. 6 | GNPS molecular network identifies carotenoid metabolites linked with genomic loci. A Molecular network of unknown features matching beta-carotene (m/z 536.4354; identified using MS/MS database) and carotene-related compounds using the Global Natural Products Social Molecular Networking. Nodes represent MS/MS spectra obtained at either discrete collision energies ranging from 10 to 50 V or stepped (SV) collision energies. The circular node shape illustrates whether features are representative ions (highest mean abundance) in clusters of co-eluting features with abundances correlating with Spearman coefficients >0.80 . Conversely, square nodes correspond to features that based on correlation with co-eluting compounds, are potentially redundant fragments or adducts. Edges

represent the cosine similarity among MS/MS spectra and formulas. Zeaxanthin is the predicted metabolite at m/z 568.427 based on m/z differences and association with *BCO1*, which catalyzes the conversion of carotenoids to retinal and *ISX*, which regulates the expression of *BCO1*. **B** Spectral comparison of plasma unknowns matching carotene and zeaxanthin MS/MS obtained using stepped and discrete collision energy, respectively, illustrating an edge cosine similarity score of 0.88. **C** Validation of compound identities for zeaxanthin and carotene confirming the retention time match of authentic standards with the unknown features in plasma (**D**) as well as their MS/MS spectrum match.

processes including regulation of blood pressure⁵¹, lipids⁵², and the development of atherosclerosis in model systems^{53–55}. Novel associations of *CD36* with plasmalogen species, which are glycerophospholipids with important antioxidant properties and have been associated with the protection of endothelial cells in hypoxic conditions⁵⁶, as well as with cell signaling and membrane stability⁵⁰, highlight potential lipid mediators, and mechanisms for the role of *CD36* in cardiometabolic disease development.

Sickle cell anemia is characterized by severe vascular abnormalities and leads to chronic cardiovascular diseases, including pulmonary hypertension, heart failure, and stroke⁵⁷. In addition, individuals with the sickle cell trait are also at increased risk of developing chronic kidney disease⁵⁸. Our findings show an association between the sickle mutation, *rs334*, and an unknown metabolite which we predict to be a lysophosphatidylcholine, a major component of red blood cell membranes. Red blood cell membrane structure is significantly altered in individuals with sickle cell disease, which affects cell shape, hemodynamics, and protein-membrane signaling interactions⁵⁹. This metabolite association may be a marker of red blood cell membrane remodeling that occurs in sickle cell disease and may help elucidate mechanisms of red blood cell pathology and resulting downstream complications of ischemic and inflammatory tissue damage.

Unknown metabolomic profiling presents an opportunity for unbiased discovery in metabolomics GWAS. However, given the breadth and diversity of the metabolome, annotating metabolite peaks with subsequent validation of proposed metabolite identities is a lengthy and arduous process, traditionally requiring extensive manual curation of study features against reference databases. To facilitate a more efficient annotation pipeline for large-scale metabolomics GWAS, we performed additional tandem MS profiling to obtain MS fragmentation data for all our peaks and implemented recently developed bioinformatic methods that leverage MS/MS spectra in metabolomics studies to help annotate unknown compounds with

chemical and/or class identities. Individual methods can help elucidate chemical identity by detailing compound sub-structure (SIRIUS), structural similarity to other metabolomic features (GNPS), and compound class (CANOPUS). In our study, no one method provided a complete annotation of study features, highlighting the challenges and complexity of working with unknown metabolomics. However, the use of complementary tools to elucidate metabolite identities enabled structural and/or class annotation for a majority of profiled peaks and represents the first systematic application of these bioinformatic tools to identify unknown peaks in a genomic association study.

We have previously demonstrated how genomic integration with MS fragmentation data on unknown metabolite peaks can help narrow the focus for these features, by mapping loci to predicted compounds based on shared metabolic pathways³⁴. Here we have systematically integrated genetic associations with MS/MS spectra-based metabolite predictions from bioinformatic techniques. We find that a majority of our metabolite annotations, based on chemical identity, can be mapped to the metabolic/functional pathway of the associated lead candidate gene, providing an additional layer of support as we decipher metabolite identities associated with cardiometabolic diseases. As an example, an unknown metabolite feature with m/z 259.1036 is associated with triglycerides, DM, and CHD among other traits in JHS (Supplementary Data 4). This metabolite peak maps to the *ATIC* gene, which encodes *5-Aminoimidazole-4-Carboxamide Ribonucleotide Formyl transferase/IMP Cyclohydrolase*, a protein-coding gene involved in purine biosynthesis. One of the top computational predictions based on tandem MS for this metabolite was AICA-Riboside (Acedesine). While this compound has been described as an AMP-activated protein kinase agonist with investigational applications in treatments for diabetes and lymphoma^{60–62}, there is evidence that endogenous levels of the compound are physiologically important. *ATIC* deficiency, a recessive genetic disease, results in impaired purine synthesis and increased urinary AICA-Riboside and is marked by severe

neurodevelopmental delays, growth impairment, and dysmorphic features^{63,64}. The association of AICA-Riboside, with its canonical enzymatic pathway in WGAS, narrowed our metabolite search to this single bioinformatic prediction, which we then confirmed with a commercial standard (Supplementary Fig. 1). Thus, the integration of genetics and MS/MS spectra can sometimes enable an efficient pipeline for identification of metabolites associated with cardiometabolic disease.

Our study represents one of the few analyses of genome-metabolome integration in a Black population. As such, validation of locus-metabolite associations presents a significant challenge, especially for associations in ancestry-specific alleles, given the scarcity of both known and unknown metabolomics profiling in Black populations. In addition, metabolomics GWAS have traditionally implemented genotype imputation of SNP array using reference panels. However, in an admixed population such as JHS, limited representative reference panels necessitate the use of more accurate imputation panels or whole genome sequencing. Further efforts to apply metabolomic profiling in Black populations and integrate with WGS will be essential to replicate key locus-metabolomic findings, though many have strong biologic plausibility. To assess the novelty of our findings, we used the most up-to-date genomic databases assessing genotype-phenotype associations, as well as a manual review of prior published metabolomics GWAS. However, there is the potential that we may have missed some previously published locus-metabolite associations. In addition, though we have made significant progress in compound identification for unknown metabolite features, a significant number still lack validation with chemical standards, and there may be some inaccuracies in chemical and/or compound class annotations, though we believe the integration of genetic findings and novel bioinformatic tools have helped minimize misclassification. While we will continue to systematically validate these compound IDs, we make available our sample library of MS/MS spectra with clinical and genomic associations, which can be leveraged across the omics community, providing a crowdsourcing opportunity for metabolite identification and serving as an ongoing resource for validation of metabolite peaks.

In summary, our integrative approach toward the identification of known and unknown metabolites involved in diverse disease processes using WGAS in a Black population highlights novel and clinically relevant locus-metabolite associations. In addition, genomic integration with advanced chemical phenotyping using tandem MS improves the ability to annotate unknown metabolite peaks, the “dark matter” of the metabolome. This sample library of MS/MS spectra of metabolite features linked to genomic loci and clinical traits will improve the identification of biologically relevant metabolites.

Methods

Cohorts

The study designs and methods for JHS, MESA, and HERITAGE have been described in refs. 65–67. JHS is a prospective population-based observational study designed to investigate risk factors for cardiovascular disease (CVD) in Black individuals. In 2000–2004, 5306 Black individuals from the Jackson, Mississippi tri-county area (Hinds, Rankin, and Madison counties) were recruited for a baseline examination. Of the original cohort, 2466 individuals had whole genome sequencing and metabolomic profiling performed from baseline fasting samples and were included in the analyses. MESA included 6814 participants between the ages of 45–84 years recruited at six clinical centers across the US, who were identified as members of four racial/ethnic groups: White, Hispanic, Asian, or Black (28%). Included in the present study are 995 individuals across all four racial/ethnic groups with metabolomic profiling and WGS at baseline exam. HERITAGE enrolled a combination of self-identified white and Black family units, totaling 763 sedentary participants (38% Black) between the ages of 17–65 years, in a 20-week, graded endurance exercise training study across

four clinical centers in the US and Canada in 1995. Included in the present study is a random subset of 658 individuals with baseline metabolomic profiling and genotyping.

Study approval

The Institutional Review Boards of Beth Israel Deaconess Medical Center, University of Mississippi Medical Center, University of Washington (MESA), and HERITAGE clinical centers approved the human study protocols, and all participants provided written informed consent.

LC-MS metabolite profiling

Metabolite profiling was performed using two LC-MS methods. Organic acids and other intermediary metabolites were separated using amide chromatography (Waters XBridge Amide column) and measured using targeted negative ion mode multiple reaction monitoring (MRM) MS with an LC-MS system comprised of an Agilent 1290 infinity LC coupled to an Agilent 6490 triple quadrupole mass spectrometer. MRM data were processed using Agilent Masshunter QQQ Quantitative analysis software⁶⁸.

Separately, amino acids, acylcarnitines, and other polar metabolites (including both known and unknown metabolite features) were separated using hydrophilic interaction liquid chromatography (HILIC) using an Atlantis HILIC column (Waters; Mildford, MA) and measured using nontargeted, full scan, high-resolution MS in the positive ion mode over m/z 70–800 with an LC-MS system comprised of a Nexera X2 U-HPLC (Shimadzu Corp.; Marlborough, MA) coupled to a Q Exactive mass spectrometer (Thermo Fisher Scientific; Waltham, MA). Raw data were processed using TraceFinder 3.3 (Thermo Fisher Scientific; Waltham, MA) for supervised integration of a subset of identified metabolites and quality control. Progenesis QI (Nonlinear Dynamics; Newcastle upon Tyne, UK) was used for the detection and integration of both identified and unknown features. Each feature in the dataset was tracked by its measured mass to charge ratio and chromatographic retention time, which serves as a unique “tag” for each LC-MS peak. Known compounds were annotated using mixtures of authentic reference standards analyzed with each batch and reference data. These metabolites had previously been annotated in human plasma and confirmed via spiking experiments with standards and by matching retention times and MS data. Metabolites with a coefficient of variation⁶⁹ greater than 30% and those missing in more than 30% of measured samples were removed from the analysis⁷⁰.

Isotope-labeled internal standards were monitored in each sample to ensure proper MS sensitivity for quality control. Pooled plasma samples were interspersed at intervals of 20 participant samples in the HILIC method and intervals of 10 participant samples in the amide chromatography method to enable correction of drift in instrument sensitivity over time and to scale data between batches. We used a linear scaling approach to the nearest pooled plasma sample in the queue. An additional pooled plasma sample was interspersed at every 20 injections to determine the coefficient of variation for each metabolite and unknown over the run. Peaks were manually reviewed in a blinded fashion to assess quality.

MS/MS data acquisition

We acquired product ion mass spectra (MS/MS) on unknown features to aid their identification. All MS/MS data were acquired using an LC-MS system comprised of a Nexera X2 U-HPLC (Shimadzu Corp.; Marlborough, MA) coupled to an ID-X orbitrap mass spectrometer (Thermo Fisher Scientific; Waltham, MA). LC conditions were identical to those used in the nontargeted HILIC method, and electrospray ionization MS settings were spray voltage 3.5 kV, sheath gas 40, sweep gas 2, capillary temperature 350 °C, heater temperature 300 °C, S-lens RF 40. MS/MS data were generated using a combination of data-dependent acquisition (DDA) and inclusion list-directed MS/MS

acquisition. For DDA, we used the AcquireX pipeline provided with the Thermo ID-X instrument and five consecutive injections of the JHS pooled plasma sample used for QC. The AcquireX scan cycle included an MS survey scan (70–800 m/z) followed by five MS/MS scans with a stepped collision energy of 10, 25, and 50 eV. To obtain MS/MS data on features not captured by the unsupervised AcquireX approach, we also used a directed MS/MS data acquisition approach in which lists of specific ions and retention time windows (inclusion lists) were created as required to measure spectra for ions of interest. First, we split all features in the study into 24 individual mass inclusion lists, separated based on ranges of metabolite peak retention times obtained from the initial LC-MS experiment, to improve the sensitivity of MS/MS data acquisition. We then generated MS/MS spectra using higher-energy C-trap dissociation (HCD) with stepped collision energies (10, 25, 50 V). Second, we targeted unknown features with GWAS hits and generated MS/MS with an expanded set of collision energies ranging from 10 to 50 V in 10 V increments. In order to increase the likelihood of capturing low abundance features in the JHS pool pooled plasma, samples used for MS/MS acquisition were concentrated ten-fold. Metabolites were extracted from 100 μL of pooled plasma using 900 μL of 74.9:24.9:0.2 (v/v/v) acetonitrile/methanol/formic acid. The samples were centrifuged (10 min, 9000 $\times g$, 4 °C) and the supernatants were dried under a gentle stream of nitrogen gas TurboVap LV, Biotage). Dried extracts were resuspended in 100 μL of 10:67.4:22.4:0.18 (v/v/v/v) water/acetonitrile/methanol/formic acid containing stable isotope-labeled internal standards (valine-d8, Sigma-Aldrich; St. Louis, MO; and phenylalanine-d8, Cambridge Isotope Laboratories; Andover, MA) and 10 μL were injected per LC-MS/MS analysis.

MS/MS data processing

Raw files were converted to *.mzML format files using MSConvert⁷¹ and both extracted ion chromatograms³⁷ and matching MS/MS scans for each individual feature were generated using the R package MSnbase v. 3.12⁷², and in-house scripts for producing EIC and MS/MS spectra visualizations. Feature retention times and peak quality in the concentrated pools were confirmed by visually inspecting the chromatography peak shapes of each individual feature. After confirming the study retention times in the MS/MS acquisition, the extraction of MS/MS data was conducted by finding scans with precursors within ± 0.2 a.m.u. of the known features and ± 0.1 min from the apex of the peak detected in the MS/MS run. Matching MS/MS peaks within 5 ppm across MS/MS scans spanning the range were aggregated whenever more than one MS/MS scan was mapped to each individual feature. The resulting peak height for aggregated peaks was determined as the average of the aggregated peak intensities. Peaks inconsistently detected across MS/MS scans were removed from the final MS/MS inventory. Additionally, an electronic noise fragment detected in the MS/MS of low abundance peaks within 30 ppm of m/z of 173.46 was removed from parsed data. Parsed MS/MS was formatted as input for molecular structure predictions (*.ms) or MS/MS-based similarity networks (*.MGF). For MS/MS-based similarity predictions, spectra generated for individual features using more than one collision energy were kept as independent molecular features.

Genotyping

Whole genome sequencing (WGS) in JHS and MESA has been described in ref. 73. Participant samples underwent $>30\times$ WGS through the Trans-Omics for Precision Medicine project at the Northwest Genome Center at the University of Washington and the Broad Institute and joint genotype calling with participants in Freeze 6; genotype calling was performed by the Informatics Resource Center at the University of Michigan. Genotyping in HERITAGE was performed on the Illumina Infinium Global Screening Array. Genotypes were called using Illumina's GenCall based on the TOP/BOT strand method. Genotype imputation to the TOPMed Freeze5 reference panel was performed using

the University of Michigan Imputation Server Minimac4. In addition, phasing was performed with Eagle v2.4. Sites with call rates $<90\%$, mismatched alleles, or invalid alleles were excluded.

Whole genome association study

Metabolite LC-MS peak areas were log-transformed and scaled to a mean of zero and standard deviation of 1 and subsequently residualized on age, sex, batch, and principal components (PCs) of ancestry 1–10 as determined by the GENetic ESTimation and Inference in Structured samples (GENESIS)⁷⁴, and subsequently inverse normalized. The association between these values and genetic variants was tested using linear mixed-effects models adjusted for age, sex, the genetic relationship matrix, and PCs 1–10 using the fastGWA model implemented in the GCTA software package⁷⁵. Variants with a minor allele count less than 5 in a given cohort were excluded from analysis in that cohort. A Bonferroni adjusted significance threshold of $8E-11$ ($5 \times 10^{-8}/602$ PC's explaining 95% of the variance of metabolite levels) was used for discovery in JHS. To identify sentinel SNPs and metabolite quantitative loci (mQTL), we first defined a 1 Mb region around each SNP significantly associated with a given metabolite. Starting at the SNP with the lowest p value, overlapping mQTLs for a particular metabolite were merged. This process was repeated until no more overlapping regions existed for the given metabolite, and the lead variant was identified as the one with the lowest p value. Lead variants that were not in overlapping regions but in linkage disequilibrium (LD) with $r^2 \geq 0.8$ were again combined using SNPClip⁷⁶, and this final merged region was designated as the mQTL, with the most significant SNP retained as the sentinel variant. Where association statistics were available in both MESA and HERITAGE, the two cohorts were meta-analyzed by the inverse-variance weighted method using the “meta-gen” package in R. Validation threshold was set at $p < 0.05$ with a consistent direction of effect.

Variant annotations

Reference allele frequencies from gnomAD and variant functional annotations using GENCODE and *ClinVar* disease annotations were obtained from the Functional Annotation of Variants—Online Resource (available favor.genohub.org, download date August 1, 2020).

Comparing to previous mQTLs

We used existing genomic databases and prior blood metabolomics GWAS to assess the novelty of our locus-metabolite associations. To determine whether mQTLs of known metabolites were novel, we first utilized the PhenoScanner package for R. A 1 MB region around each sentinel SNP associated with a metabolite was passed to the PhenoScanner function in R: build was set to “38”, p value to 5×10^{-8} , catalog to “mQTL” (query date 12/1/2021). Novel locus-metabolite associations were cross-referenced against the GWAS Catalogue using the sentinel SNP and a 1 MB surrounding region. In addition, gene-metabolite associations were manually reviewed for novelty across 21 published GWAS of metabolomics (details of individual studies reviewed in Supplementary Methods)^{3–23}.

mQTL and phenotype associations

To determine overlap between clinical GWAS analyses and mQTLs in this analysis, we utilized the PhenoScanner package for R. All sentinel SNPs associated with metabolite peaks as identified above were passed to the PhenoScanner function in R with the following arguments: build was set to “38”, p value to 1×10^{-5} , catalog to “GWAS”, r^2 was set to “0.8”, proxies set to “None” (query date 12/1/2021).

Unknown metabolite peak annotation

Metabolite peak clustering. The electrospray ionization process used in LC-MS can generate more than one type of ion adduct of a molecule (e.g., $[M + H]^+$, $[M + Na]^+$, etc.), partially fragment molecules, and

generate multimer ions. A single metabolite may therefore give rise to multiple unknown peaks. However, such redundant features share the same chromatographic retention time and have highly correlated signal intensities. To filter redundant features, all profiled metabolite peaks (HILIC platform) were grouped into clusters based on a retention time similarity of ± 0.25 min and a signal intensity spearman correlation coefficient > 0.80 . The $[M+H]^+$ ion, if identified by mass differences among features in the cluster or the feature with the highest signal intensity, was identified as the primary feature.

Metabolite annotations leveraging MS/MS spectra and bioinformatic tools. Parsed MS/MS data (*.ms) were loaded into SIRIUS CSI-Finger ID version 4.7.2⁴⁰. Molecular formula predictions generated with Orbitrap-specific settings (MS/MS isotope scorer: ignore, mass deviation: 5 ppm, Candidates: 10, Candidates per ion: 1, possible ionizations: $[M+H]^+$, $[M+K]^+$, $[M+Na]^+$). Structure elucidations were done using PubChem and the adducts $[M+H]^+$, $[M+K]^+$, $[M+Na]^+$. Predictions were exported and the top three structure elucidations were parsed for each feature. Parsed MS/MS data for each metabolite peak were annotated for predicted metabolite class using ClassyFire ontology through CANOPUS³⁹. MS/MS-based networks were built using the Global Natural Products Social Molecular Networking (GNPS)⁴¹, and the resulting networks were visualized with Cytoscape v. 3.8.2⁷⁷. To provide supporting information for our metabolite annotations, we searched the Human Metabolome database with $m/z \pm 5$ ppm³².

Metabolite annotation scheme. Results from metabolite feature clustering, class, and chemical structure elucidations were integrated to annotate metabolite peaks. We subsequently assigned each annotation to a category based on levels of supporting evidence. In addition, we classified the categories of metabolite identification in accordance with the Metabolomics Standards Initiative (MSI) recommendations (Supplementary Table 2):⁷⁸ Category 1: metabolite match to an authentic reference standard; Category 2: metabolite clusters with a known compound which has previously validated with standard (Category 1 and 2 corresponds to MSI Classification 1 as Identified Metabolite); Category 3: metabolite with MS/MS-based GNPS database match (MSI Classification 2: putatively annotated metabolite); Category 4: Metabolite with similar MS/MS spectra and retention time with the representative backbone of chemical standard for a compound in the metabolite family (manual curation) using in-house metabolite library (MSI classification 3: putatively annotated metabolite class). In addition, we add category 5: SIRIUS MS/MS-based chemical formula/compound predictions and Category 6: compound match using m/z search in HMDB, which are not included in the 2007 MSI classification scheme. Primary unknown metabolites with multiple sources of supporting evidence represented high-confidence metabolite annotations and were assigned specific metabolite IDs.

Genomic and metabolite pathway integration. Genetic associations with unknown metabolite peaks can be integrated with MS/MS and bioinformatic metabolite annotations in an effort to further illuminate metabolite identifications and/or offer supporting evidence for predictions based on the known pathways of the locus. Each lead candidate gene (nearest gene to sentinel SNP) was annotated for its associated metabolic pathways using the KEGG database⁷⁹. Metabolite annotations were evaluated in the context of the metabolic pathways of the candidate gene or its prior GWAS associations to assess whether there was genomic evidence in support of the chemical compound identification.

Reporting summary

Further information on research design is available in the Nature Research Reporting Summary linked to this article.

Data availability

The WGAS summary statistics data generated in this study have been deposited in the GWAS catalog under accession code [GCST90104476](https://www.ebi.ac.uk/gwas/studies/GCST90104476). Individual WGS data for TOPMed and metabolomic data for JHS and MESA, can be obtained by application to dbGaP with accession numbers for JHS and MESA are [phs000964](https://www.ncbi.nlm.nih.gov/geo/query/acc.cgi?acc=phs000964)/[phs002256](https://www.ncbi.nlm.nih.gov/geo/query/acc.cgi?acc=phs002256).v5.p1 and [phs001416](https://www.ncbi.nlm.nih.gov/geo/query/acc.cgi?acc=phs001416).v2.p1. In addition, MS/MS spectra and analyses via Global Natural Product Structural Molecular Networking (GNPS) Job ID: [aad6d11c8be15436abcb7d3d44fee5836](https://www.ebi.ac.uk/gnps/job/aad6d11c8be15436abcb7d3d44fee5836) can be accessed at.

References

1. McGarrah, R. W., Crown, S. B., Zhang, G.-F., Shah, S. H. & Newgard, C. B. Cardiovascular metabolomics. *Circ. Res.* **122**, 1238–1258 (2018).
2. Spratlin, J. L., Serkova, N. J. & Eckhardt, S. G. Clinical applications of metabolomics in oncology: a review. *Clin. Cancer Res.* **15**, 431–440 (2009).
3. Gerszten, R. E. & Wang, T. J. The search for new cardiovascular biomarkers. *Nature* **451**, 949–952 (2008).
4. Gieger, C. et al. Genetics meets metabolomics: a genome-wide association study of metabolite profiles in human serum. *PLoS Genet.* **4**, e1000282 (2008).
5. Hicks, A. A. et al. Genetic determinants of circulating sphingolipid concentrations in European populations. *PLoS Genet.* **5**, e1000672 (2009).
6. Illig, T. et al. A genome-wide perspective of genetic variation in human metabolism. *Nat. Genet.* **42**, 137–141 (2010).
7. Lemaitre, R. N. et al. Genetic loci associated with plasma phospholipid n-3 fatty acids: a meta-analysis of genome-wide association studies from the CHARGE Consortium. *PLoS Genet.* **7**, e1002193 (2011).
8. Suhre, K. et al. Human metabolic individuality in biomedical and pharmaceutical research. *Nature* **477**, 54–60 (2011).
9. Suhre, K. et al. A genome-wide association study of metabolic traits in human urine. *Nat. Genet.* **43**, 565–569 (2011).
10. Tukiainen, T. et al. Detailed metabolic and genetic characterization reveals new associations for 30 known lipid loci. *Hum. Mol. Genet.* **21**, 1444–1455 (2011).
11. Demirkan, A. et al. Genome-wide association study identifies novel loci associated with circulating phospho- and sphingolipid concentrations. *PLoS Genet.* **8**, e1002490 (2012).
12. Inouye, M. et al. Novel loci for metabolic networks and multi-tissue expression studies reveal genes for atherosclerosis. *PLoS Genet.* **8**, e1002907 (2012).
13. Kettunen, J. et al. Genome-wide association study identifies multiple loci influencing human serum metabolite levels. *Nat. Genet.* **44**, 269–276 (2012).
14. Krumsiek, J. et al. Mining the unknown: a systems approach to metabolite identification combining genetic and metabolic information. *PLoS Genet.* **8**, e1003005 (2012).
15. Shin, S.-Y. et al. An atlas of genetic influences on human blood metabolites. *Nat. Genet.* **46**, 543–550 (2014).
16. Yu, B. et al. Genetic determinants influencing human serum metabolome among African Americans. *PLoS Genet.* **10**, e1004212 (2014).
17. Burkhardt, R. et al. Integration of genome-wide SNP data and gene-expression profiles reveals six novel loci and regulatory mechanisms for amino acids and acylcarnitines in whole blood. *PLoS Genet.* **11**, e1005510 (2015).
18. Demirkan, A. et al. Insight in genome-wide association of metabolite quantitative traits by exome sequence analyses. *PLoS Genet.* **11**, e1004835 (2015).
19. Draisma, H. H. M. et al. Genome-wide association study identifies novel genetic variants contributing to variation in blood metabolite levels. *Nat. Commun.* **6**, 7208 (2015).

20. Rhee, E. P. et al. An exome array study of the plasma metabolome. *Nat. Commun.* **7**, 12360 (2016).
21. Long, T. et al. Whole-genome sequencing identifies common-to-rare variants associated with human blood metabolites. *Nat. Genet.* **49**, 568–578 (2017).
22. Yazdani, A. et al. Genome analysis and pleiotropy assessment using causal networks with loss of function mutation and metabolomics. *BMC Genomics* **20**, 395 (2019).
23. Lotta, L. A. et al. A cross-platform approach identifies genetic regulators of human metabolism and health. *Nat. Genet.* **53**, 54–64 (2021).
24. Raffler, J. et al. Identification and MS-assisted interpretation of genetically influenced NMR signals in human plasma. *Genome Med.* **5**, 13 (2013).
25. Baldassari, A. R. et al. Multi-ethnic genome-wide association study of decomposed cardioelectric phenotypes illustrates strategies to identify and characterize evidence of shared genetic effects for complex traits. *Circ. Genom. Precis. Med.* **13**, e002680 (2020).
26. Roselli, C. et al. Multi-ethnic genome-wide association study for atrial fibrillation. *Nat. Genet.* **50**, 1225–1233 (2018).
27. Wyss, A. B. et al. Multiethnic meta-analysis identifies ancestry-specific and cross-ancestry loci for pulmonary function. *Nat. Commun.* **9**, 2976 (2018).
28. McClellan, J. M., Lehner, T. & King, M.-C. Gene discovery for complex traits: lessons from Africa. *Cell* **171**, 261–264 (2017).
29. Stein, E. A. et al. Effect of a monoclonal antibody to PCSK9 on LDL cholesterol. *N. Engl. J. Med.* **366**, 1108–1118 (2012).
30. Menni, C. et al. Biomarkers for type 2 diabetes and impaired fasting glucose using a nontargeted metabolomics approach. *Diabetes* **62**, 4270–4276 (2013).
31. Sévin, D. C., Kuehne, A., Zamboni, N. & Sauer, U. Biological insights through nontargeted metabolomics. *Curr. Opin. Biotechnol.* **34**, 1–8 (2015).
32. Wishart, D. S. et al. HMDB: the human metabolome database. *Nucleic Acids Res.* **35**, D521–D526 (2007).
33. Zang, X., Monge, M. E. & Fernández, F. M. Mass spectrometry-based non-targeted metabolic profiling for disease detection: recent developments. *Trends Anal. Chem.* **118**, 158–169 (2019).
34. O’Sullivan, J. F. et al. Dimethylguanidino valeric acid is a marker of liver fat and predicts diabetes. *J. Clin. Invest.* **127**, 4394–4402 (2017).
35. Staley, J. R. et al. PhenoScanner: a database of human genotype-phenotype associations. *Bioinformatics* **32**, 3207–3209 (2016).
36. Buniello, A. et al. The NHGRI-EBI GWAS Catalog of published genome-wide association studies, targeted arrays and summary statistics 2019. *Nucleic Acids Res.* **47**, D1005–d1012 (2019).
37. Karczewski, K. J. et al. The mutational constraint spectrum quantified from variation in 141,456 humans. *Nature* **581**, 434–443 (2020).
38. Gold, L. et al. Aptamer-based multiplexed proteomic technology for biomarker discovery. *PLoS ONE* **5**, e15004 (2010).
39. Dührkop, K. et al. Systematic classification of unknown metabolites using high-resolution fragmentation mass spectra. *Nat. Biotechnol.* **39**, 462–471 (2021).
40. Dührkop, K. et al. SIRIUS 4: a rapid tool for turning tandem mass spectra into metabolite structure information. *Nat. Methods* **16**, 299–302 (2019).
41. Wang, M. et al. Sharing and community curation of mass spectrometry data with Global Natural Products Social Molecular Networking. *Nat. Biotechnol.* **34**, 828–837 (2016).
42. Yang, X. et al. SCARB1 gene variants are associated with the phenotype of combined high high-density lipoprotein cholesterol and high lipoprotein (a). *Circ Cardiovasc. Genet.* **9**, 408–418 (2016).
43. van Bennekum, A. et al. Class B scavenger receptor-mediated intestinal absorption of dietary β -carotene and cholesterol. *Biochemistry* **44**, 4517–4525 (2005).
44. Widjaja-Adhi, M. A. K. et al. Transcription factor ISX mediates the cross talk between diet and immunity. *Proc. Natl Acad. Sci. USA* **114**, 11530–11535 (2017).
45. Arvanitis, M. et al. Identification of transthyretin cardiac amyloidosis using serum retinol-binding protein 4 and a clinical prediction model. *JAMA Cardiol.* **2**, 305–313 (2017).
46. Hauser, P. S., Narayanaswami, V. & Ryan, R. O. Apolipoprotein E: from lipid transport to neurobiology. *Prog. Lipid Res.* **50**, 62–74 (2011).
47. van Duijn, C. M. et al. Apolipoprotein E4 allele in a population-based study of early-onset Alzheimer’s disease. *Nat. Genet.* **7**, 74–78 (1994).
48. Grimm, M. O. W., Mett, J. & Hartmann, T. The impact of vitamin E and other fat-soluble vitamins on Alzheimer’s disease. *Int J. Mol. Sci.* **17**, 1785 (2016).
49. Jiménez-Jiménez, F. J. et al. Cerebrospinal fluid levels of alpha-tocopherol (vitamin E) in Alzheimer’s disease. *J. Neural Transm.* **104**, 703–710 (1997).
50. Omi, K. et al. CD36 polymorphism is associated with protection from cerebral malaria. *Am. J. Hum. Genet.* **72**, 364–374 (2003).
51. Pravenec, M. et al. Identification of renal Cd36 as a determinant of blood pressure and risk for hypertension. *Nat. Genet.* **40**, 952–954 (2008).
52. Kuwasako, T. et al. Lipoprotein abnormalities in human genetic CD36 deficiency associated with insulin resistance and abnormal fatty acid metabolism. *Diabetes Care* **26**, 1647–1648 (2003).
53. Park, Y. M. CD36, a scavenger receptor implicated in atherosclerosis. *Exp. Mol. Med.* **46**, e99–e99 (2014).
54. Febbraio, M., Hajjar, D. P. & Silverstein, R. L. CD36: a class B scavenger receptor involved in angiogenesis, atherosclerosis, inflammation, and lipid metabolism. *J. Clin. Invest.* **108**, 785–791 (2001).
55. Moore, K. J. & Freeman, M. W. Scavenger receptors in atherosclerosis. *Arterioscler. Thromb. Vasc. Biol.* **26**, 1702–1711 (2006).
56. Zoeller, R. A. et al. Increasing plasmalogen levels protects human endothelial cells during hypoxia. *Am. J. Physiol. Heart Circ. Physiol.* **283**, H671–H679 (2002).
57. Ranque, B. et al. Arterial stiffness impairment in sickle cell disease associated with chronic vascular complications. *Circulation* **134**, 923–933 (2016).
58. Gladwin, M. T. & Sachdev, V. Cardiovascular abnormalities in sickle cell disease. *J. Am. Coll. Cardiol.* **59**, 1123–1133 (2012).
59. Liu, S. C. et al. Red cell membrane remodeling in sickle cell anemia. Sequestration of membrane lipids and proteins in Heinz bodies. *J. Clin. Invest.* **97**, 29–36 (1996).
60. Vincent, M. F., Marangos, P. J., Gruber, H. E. & Van den Berghe, G. Inhibition by AICA riboside of gluconeogenesis in isolated rat hepatocytes. *Diabetes* **40**, 1259–1266 (1991).
61. Campàs, C., Santidrián, A. F., Domingo, A. & Gil, J. Acadesine induces apoptosis in B cells from mantle cell lymphoma and splenic marginal zone lymphoma. *Leukemia* **19**, 292–294 (2005).
62. Santidrián, A. F. et al. AICAR induces apoptosis independently of AMPK and p53 through up-regulation of the BH3-only proteins BIM and NOXA in chronic lymphocytic leukemia cells. *Blood* **116**, 3023–3032 (2010).
63. Marie, S. et al. AICA-ribosiduria: a novel, neurologically devastating inborn error of purine biosynthesis caused by mutation of ATIC. *Am. J. Hum. Genet.* **74**, 1276–1281 (2004).
64. Ramond, F. et al. AICA-ribosiduria due to ATIC deficiency: delineation of the phenotype with three novel cases, and long-term update on the first case. *J. Inher. Metab. Dis.* **43**, 1254–1264 (2020).
65. Taylor, H. A. Jr. et al. Toward resolution of cardiovascular health disparities in African Americans: design and methods of the Jackson Heart Study. *Ethn. Dis.* **15**, S6–4–17 (2005).
66. Bild, D. E. et al. Multi-ethnic study of atherosclerosis: objectives and design. *Am. J. Epidemiol.* **156**, 871–881 (2002).

67. Bouchard, C. et al. The HERITAGE family study. Aims, design, and measurement protocol. *Med Sci. Sports Exerc.* **27**, 721–729 (1995).
68. Tahir, U. A. et al. Metabolomic profiles and heart failure risk in black adults: insights from the Jackson Heart Study. *Circ. Heart Fail.* **14**, e007275 (2021).
69. Bar, N. et al. A reference map of potential determinants for the human serum metabolome. *Nature* **588**, 135–140 (2020).
70. Do, K. T. et al. Characterization of missing values in untargeted MS-based metabolomics data and evaluation of missing data handling strategies. *Metabolomics* **14**, 128–128 (2018).
71. Chambers, M. C. et al. A cross-platform toolkit for mass spectrometry and proteomics. *Nat. Biotechnol.* **30**, 918–920 (2012).
72. Gatto, L. & Lilley, K. S. MSnbase-an R/Bioconductor package for isobaric tagged mass spectrometry data visualization, processing and quantitation. *Bioinformatics* **28**, 288–289 (2012).
73. Raffield, L. M. et al. D-dimer in African Americans: whole genome sequence analysis and relationship to cardiovascular disease risk in the Jackson Heart Study. *Arterioscler. Thromb. Vasc. Biol.* **37**, 2220–2227 (2017).
74. Conomos, M. P., Miller, M. B. & Thornton, T. A. Robust inference of population structure for ancestry prediction and correction of stratification in the presence of relatedness. *Genet. Epidemiol.* **39**, 276–293 (2015).
75. Jiang, L. et al. A resource-efficient tool for mixed model association analysis of large-scale data. *Nat. Genet.* **51**, 1749–1755 (2019).
76. Myers, T. A., Chanock, S. J. & Machiela, M. J. LDlinkR: an R package for rapidly calculating linkage disequilibrium statistics in diverse populations. *Front. Genet.* **11**, 157 (2020).
77. Otasek, D., Morris, J. H., Bouças, J., Pico, A. R. & Demchak, B. Cytoscape automation: empowering workflow-based network analysis. *Genome Biol.* **20**, 185 (2019).
78. Sumner, L. W. et al. Proposed minimum reporting standards for chemical analysis Chemical Analysis Working Group (CAWG) Metabolomics Standards Initiative (MSI). *Metabolomics* **3**, 211–221 (2007).
79. Kanehisa, M. & Goto, S. KEGG: kyoto encyclopedia of genes and genomes. *Nucleic Acids Res.* **28**, 27–30 (2000).

Acknowledgements

Dr. Tahir is supported by the John S. LaDue Memorial Fellowship in Cardiology. Dr. Katz is supported by an NHLBI T32 post-doctoral training grant (T32HL007374-O). Dr. Cruz is supported by the KL2/Catalyst Medical Research Investigator Training award from Harvard Catalyst (NIH/NCATS Award TR002542). Dr. Robbins is supported by the NHLBI K23HL150327 award. Dr. Benson is supported by the NHLBI K08HL145095 award. Dr. Ruberg is supported by NIH R01HL139671. Dr. Natarajan is supported by grants from the NHLBI (R01HL142711, R01HL148050, R01HL151283, R01HL127564, R01HL148565, R01HL135242, and R01HL151152), Fondation Leducq (TNE-18CVD04), and Massachusetts General Hospital (Paul & Phyllis Fireman Endowed Chair in Vascular Medicine). Drs. Gerszten, Wang, and Wilson are supported by NIH R01 DK081572.

The Jackson Heart Study (JHS) is supported and conducted in collaboration with Jackson State University (HHSN268201800013I), Tougaloo College (HHSN268201800014I), the Mississippi State Department of Health (HHSN268201800015I/HHSN26800001) and the University of Mississippi Medical Center (HHSN268201800010I, HHSN268201800011I, and HHSN268201800012I) contracts from the National Heart, Lung, and Blood Institute⁷³ and the National Institute for Minority Health and Health Disparities (NIMHD). Molecular data for the Trans-Omics in Precision Medicine (TOPMed) program was supported by the National Heart, Lung and Blood Institute⁷³. Genome sequencing for “NHLBI TOPMed: The Jackson Heart Study” (phs000964.v1.p1) was performed at the Northwest Genomics Center (HHSN268201100037C). Core support, including centralized genomic read mapping and

genotype calling, along with variant quality metrics and filtering were provided by the TOPMed Informatics Research Center (3R01HL-117626-02S1; contract HHSN268201800002I). Core support, including phenotype harmonization, data management, sample-identity QC, and general program coordination, were provided by the TOPMed Data Coordinating Center (R01HL-120393; U01HL-120393; contract HHSN268201800001I) and the TOPMed Centralized Omics Resource (CORE; contract HHSN268201600034I). We gratefully acknowledge the studies and participants who provided biological samples and data for TOPMed. The authors wish to thank the staff and participants of the JHS.

We thank Drs. Arthur S. Leon, D.C. Rao, James S. Skinner, Tuomo Rankinen, Jacques Gagnon, and the late Jack H. Wilmore for contributions to the planning, data collection, and conduct of the HERITAGE project. This research was partially funded by National Heart, Lung, and Blood Institute Grants HL-45670, HL-47317, HL-47321, HL-47323, and HL-47327, to Dr. Bouchard and his colleagues all in support of the HERITAGE Family Study. C.B. is partially funded by the John W. Barton Sr. Chair in Genetics and Nutrition, and NIH COBRE grant (NIH P30GM118430-01). Dr. Sarzynski is supported by R01HL146462.

TOPMed MESA Multi-Omics/MESA Study Acknowledgement

Whole genome sequencing (WGS) for the Trans-Omics in Precision Medicine program was supported by the National Heart, Lung and Blood Institute. WGS for “NHLBI TOPMed: Multi-Ethnic Study of Atherosclerosis (MESA)” (phs001416.v1.p1) was performed at the Broad Institute of MIT and Harvard (3U54HG003067-13S1). Centralized read mapping and genotype calling, along with variant quality metrics and filtering, were provided by the TOPMed Informatics Research Center (3R01HL-117626-02S1). Phenotype harmonization, data management, sample-identity QC, and general study coordination were provided by the TOPMed Data Coordinating Center (3R01HL-120393-02S1). The MESA projects are conducted and supported by the National Heart, Lung, and Blood Institute in collaboration with MESA investigators. Support for the Multi-Ethnic Study of Atherosclerosis (MESA) projects are conducted and supported by the National Heart, Lung, and Blood Institute in collaboration with MESA investigators. Support for MESA is provided by contracts 75N92020D00001, HHSN268201500003I, N01-HC-95159, 75N92020D00005, N01-HC-95160, 75N92020D00002, N01-HC-95161, 75N92020D00003, N01-HC-95162, 75N92020D00006, N01-HC-95163, 75N92020D00004, N01-HC-95164, 75N92020D00007, N01-HC-95165, N01-HC-95166, N01-HC-95167, N01-HC-95168, N01-HC-95169, UL1-TR-000040, UL1-TR-001079, and UL1-TR-001420, UL1TR001881, DK063491, and R01HL105756. The authors thank the other investigators, the staff, and the participants of the MESA study for their valuable contributions. A full list of participating MESA investigators and institutes can be found at <http://www.mesa-nhlbi.org>.

The views expressed in this manuscript are those of the authors and do not necessarily represent the views of the National Heart, Lung, and Blood Institute; the National Institutes of Health; or the U.S. Department of Health and Human Services.

Author contributions

U.A.T., D.H.K., J.A.-P., A.G.B., T.J.W., J.G.W., C.B.P., P.N., and R.E.G. contributed to the original concept of the project, planned these analyses, and formulated the methods. D.H.K., U.A.T., D.N., M.D.B., Z.Z.C., J.M.R., D.E.C., SD, L.F., S.S.R., M.E.H., A.C., J.G.W., and R.E.G., collected, organized, and contributed to the quality control and management of JHS metabolomics data. D.H.K., U.A.T., X.S., S.Z., D.N., M.D.B., J.M.R., D.E.C., S.D., L.F., S.S.R., D.S., R.P.T., P.D., K.D.T., Y.L., W.C.J., X.G., J.Y., Y.-D.I.C., A.W.M., S.S.R., J.I.R., and R.E.G., collected, generated, organized, and contributed to the quality control and management of MESA metabolomics data. D.H.K., U.A.T., D.N., M.D.B., J.M.R., D.E.C., S.D., L.F., S.S., D.S., C.B., M.A.S., and R.E.G. collected, generated, organized, and contributed to the quality control and management of HERITAGE Family Study metabolomics and genomic data. F.L.R and W.S.B contributed to the validation of unknown metabolite identities. D.J. and TOPMed

performed W.G.S. from JHS and MESA. D.H.K., U.A.T, A.G.B, A.P., Z.Y., A.E., S.D., P.N., and R.E.G. developed the WGS analysis pipeline and statistical methods across all metabolomics data. D.H.K., U.A.T., J.A.-P., C.B.C., P.N., and R.E.G. analyzed the data and wrote/revised the article.

Competing interests

A.G.B. is a co-founder and shareholder of TenSixteen Bio. P.N. reports personal consulting fees from Amgen, Apple, AstraZeneca, Genentech/Roche, Novartis, TenSixteen Bio, Foresite Labs, and Blackstone Life Sciences, grant support from Amgen, Apple, AstraZeneca, Boston Scientific, and Novartis, is a scientific advisory board member with equity of TenSixteen Bio and geneXwell, and spousal support and equity in Vertex, all unrelated to the present work; P.N.'s interests were reviewed and are managed by Massachusetts General Hospital and Mass General Brigham in accordance with their conflict of interest policies. The remaining authors declare no competing interests.

Additional information

Supplementary information The online version contains supplementary material available at <https://doi.org/10.1038/s41467-022-32275-3>.

Correspondence and requests for materials should be addressed to Robert E. Gerszten.

Peer review information *Nature Communications* thanks the anonymous reviewers for their contribution to the peer review of this work.

Reprints and permission information is available at <http://www.nature.com/reprints>

Publisher's note Springer Nature remains neutral with regard to jurisdictional claims in published maps and institutional affiliations.

Open Access This article is licensed under a Creative Commons Attribution 4.0 International License, which permits use, sharing, adaptation, distribution and reproduction in any medium or format, as long as you give appropriate credit to the original author(s) and the source, provide a link to the Creative Commons license, and indicate if changes were made. The images or other third party material in this article are included in the article's Creative Commons license, unless indicated otherwise in a credit line to the material. If material is not included in the article's Creative Commons license and your intended use is not permitted by statutory regulation or exceeds the permitted use, you will need to obtain permission directly from the copyright holder. To view a copy of this license, visit <http://creativecommons.org/licenses/by/4.0/>.

© The Author(s) 2022

¹Division of Cardiovascular Medicine, Beth Israel Deaconess Medical Center, Harvard Medical School, Boston, MA, US. ²Broad Institute of Harvard and MIT, Cambridge, MA, US. ³University of Mississippi Medical Center, Jackson, MS, US. ⁴Department of Pathology Laboratory Medicine, Larner College of Medicine, University of Vermont, Burlington, VT, US. ⁵The Institute for Translational Genomics and Population Sciences, Department of Pediatrics, The Lundquist Institute for Biomedical Innovation at Harbor UCLA Medical Center, Torrance, CA, US. ⁶Department of Medicine, Division of Cardiology, Duke Molecular Physiology Institute, Duke University Medical Center, Durham, NC, US. ⁷Department of Biostatistics, University of Washington, Seattle, WA, US. ⁸Center for Public Health Genomics, University of Virginia, Charlottesville, Virginia, US. ⁹Division of Biostatistics and Epidemiology, Department of Public Health Sciences, University of Virginia, Charlottesville, Virginia, US. ¹⁰Section of Cardiovascular Medicine, Boston University School of Medicine and Boston Medical Center, Boston, MA, US. ¹¹Columbia University Medical Center, New York, NY, US. ¹²University of Washington, Seattle, Washington, US. ¹³Human Genomic Laboratory, Pennington Biomedical Research Center, Baton Rouge, LA, US. ¹⁴Department of Exercise Science, University of South Carolina, Columbia, SC, US. ¹⁵Department of Medicine, UT Southwestern Medical Center, Dallas, TX, US. ¹⁶Cardiovascular Research Center, Massachusetts General Hospital, Harvard Medical School, Boston, MA, US. ¹⁸⁵These authors contributed equally: Usman A. Tahir, Daniel H. Katz, Julian Avila-Pachecho, Clary B. Clish, Pradeep Natarajan, Robert E. Gerszten. *A list of authors and their affiliations appears at the end of the paper. ✉e-mail: rgerszte@bidmc.harvard.edu

NHLBI Trans-Omics for Precision Medicine 1 Consortium

Namiko Abe¹⁷, Gonçalo Abecasis¹⁸, Francois Aguet¹⁹, Christine Albert²⁰, Laura Almasy²¹, Alvaro Alonso²², Seth Ament²³, Peter Anderson¹², Pramod Anugu²⁴, Deborah Applebaum-Bowden²⁵, Kristin Ardlie¹⁹, Dan Arking²⁶, Donna K. Arnett²⁷, Allison Ashley-Koch²⁸, Stella Aslibekyan²⁹, Tim Assimes³⁰, Paul Auer³¹, Dimitrios Avramopoulos²⁶, Najib Ayas³², Adithya Balasubramanian³³, John Barnard³⁴, Kathleen Barnes³⁵, R. Graham Barr³⁶, Emily Barron-Casella²⁶, Lucas Barwick³⁷, Terri Beaty²⁶, Gerald Beck³⁸, Diane Becker³⁹, Lewis Becker²⁶, Rebecca Beer⁴⁰, Amber Beitelshees²³, Emelia Benjamin⁴¹, Takis Benos⁴², Marcos Bezerra⁴³, Larry Bielak¹⁸, Joshua Bis⁴⁴, Thomas Blackwell¹⁸, John Blangero⁴⁵, Nathan Blue⁴⁶, Eric Boerwinkle⁴⁷, Donald W. Bowden⁴⁸, Russell Bowler⁴⁹, Jennifer Brody¹², Ulrich Broeckel⁵⁰, Jai Broome¹², Deborah Brown⁵¹, Karen Bunting¹⁷, Esteban Burchard⁵², Carlos Bustamante⁵³, Erin Buth⁷, Brian Cade⁵⁴, Jonathan Cardwell⁵⁵, Vincent Carey⁵⁶, Julie Carrier⁵⁷, April Carson⁵⁸, Cara Carty⁵⁹, Richard Casaburi⁶⁰, Juan P. Casas Romero⁵⁶, James Casella²⁶, Peter Castaldi⁶¹, Mark Chaffin¹⁹, Christy Chang²³, Yi-Cheng Chang⁶², Daniel Chasman⁶³, Sameer Chavan⁵⁵, Bo-Juen Chen¹⁷, Wei-Min Chen⁶⁴, Michael Cho⁵⁶, Seung Hoan Choi¹⁹, Lee-Ming Chuang⁶⁵, Mina Chung³⁴, Ren-Hua Chung⁶⁶, Suzy Comhair⁶⁷, Matthew Conomos⁷, Elaine Cornell⁶⁸, Carolyn Crandall⁶⁰, James Crapo⁴⁹, L. Adrienne Cupples⁶⁹, Joanne Curran⁷⁰, Jeffrey Curtis⁷¹, Brian Custer⁷², Coleen Dancott²³, Dawood Darbar⁷³, Sean David⁷⁴, Colleen Davis¹², Michelle Daya⁵⁵, Mariza de Andrade⁷⁵, Lisa de las Fuentes⁷⁶, Paul de Vries⁷⁷, Michael DeBaun⁷⁸, Ranjan Deka⁷⁹, Dawn DeMeo⁵⁶, Scott Devine²³, Huyen Dinh³³, Harsha Doddapaneni³³, Qing Duan⁸⁰, Shannon Dugan-Perez³³, Ravi Duggirala⁸¹, Susan K. Dutcher⁸², Charles Eaton⁸³, Lynette Ekunwe²⁴, Adel El Boueiz⁸⁴, Patrick Ellinor⁸⁵, Leslie Emery¹², Serpil Erzurum³⁴, Charles Farber⁶⁴, Jesse Farek³³, Tasha Fingerlin⁸⁶, Matthew Flickinger¹⁸, Myriam Fornage⁴⁷, Nora Franceschini⁸⁷, Chris Frazar¹², Mao Fu²³,

Stephanie M. Fullerton¹², Lucinda Fulton⁸⁸, Stacey Gabriel¹⁹, Weiniu Gan⁴⁰, Shanshan Gao⁵⁵, Yan Gao²⁴, Margery Gass⁸⁹, Heather Geiger¹⁷, Bruce Gelb⁹⁰, Mark Geraci⁴², Soren Germer¹⁷, Auyon Ghosh⁵⁶, Richard Gibbs³³, Chris Gignoux³⁰, Mark Gladwin⁴², David Glahn⁹¹, Stephanie Gogarten¹², Da-Wei Gong²³, Harald Goring⁹², Sharon Graw⁹³, Kathryn J. Gray⁹⁴, Daniel Grine⁵⁵, Colin Gross¹⁸, C. Charles Gu⁸⁸, Yue Guan²³, Namrata Gupta¹⁹, Jeff Haessler⁸⁹, Yi Han³³, Patrick Hanly⁹⁵, Daniel Harris⁹⁶, Nicola L. Hawley⁹⁷, Jiang He⁹⁸, Ben Heavner⁷, Susan Heckbert⁹⁹, Ryan Hernandez⁵², David Herrington¹⁰⁰, Craig Hersh¹⁰¹, Bertha Hidalgo²⁹, James Hixson⁴⁷, Brian Hobbs⁵⁶, John Hokanson⁵⁵, Elliott Hong²³, Karin Hoth¹⁰², Chao Hsiung^{66,103}, Jianhong Hu³³, Yi-Jen Hung¹⁰⁴, Haley Huston¹⁰⁵, Chii Min Hwu¹⁰⁶, Marguerite Ryan Irvin²⁹, Rebecca Jackson¹⁰⁷, Cashell Jaquish⁴⁰, Jill Johnsen¹⁰⁸, Andrew Johnson⁴⁰, Rich Johnston²², Kimberly Jones²⁶, Hyun Min Kang¹⁰⁹, Robert Kaplan¹¹⁰, Sharon Kardia¹⁸, Shannon Kelly¹¹¹, Eimear Kenny⁹⁰, Michael Kessler²³, Alyna Khan¹², Ziad Khan³³, Wonji Kim¹¹², John Kimoff¹¹³, Greg Kinney¹¹⁴, Barbara Konkle¹¹⁵, Charles Kooperberg⁸⁹, Holly Kramer¹¹⁶, Christoph Lange¹¹⁷, Ethan Lange⁵⁵, Leslie Lange¹¹⁸, Cathy Laurie¹², Cecelia Laurie¹², Meryl LeBoff⁵⁶, Jiwon Lee⁵⁶, Sandra Lee³³, Wen-Jane Lee¹⁰⁶, Jonathon LeFaive¹⁸, David Levine¹², Dan Levy⁴⁰, Joshua Lewis²³, Xiaohui Li¹¹⁹, Yun Li⁸⁰, Henry Lin¹¹⁹, Honghuang Lin¹²⁰, Xihong Lin¹²¹, Simin Liu¹²², Yu Liu¹²³, Ruth J. F. Loos¹²⁴, Steven Lubitz⁸⁵, Kathryn Lunetta¹²⁵, James Luo⁴⁰, Ulysses Magalang¹²⁶, Michael Mahaney⁷⁰, Barry Make²⁶, Alisa Manning¹²⁷, JoAnn Manson⁵⁶, Lisa Martin¹²⁸, Melissa Marton¹⁷, Susan Mathai⁵⁵, Rasika Mathias²⁶, Susanne May⁷, Patrick McArdle²³, Merry-Lynn McDonald²⁹, Sean McFarland¹¹², Stephen McGarvey¹²⁹, Daniel McGoldrick¹³⁰, Caitlin McHugh⁷, Becky McNeil¹³¹, Hao Mei²⁴, James Meigs¹³², Vipin Menon³³, Luisa Mestroni⁹³, Ginger Metcalf³³, Deborah A. Meyers¹³³, Emmanuel Mignot¹³⁴, Julie Mikulla⁴⁰, Nancy Min²⁴, Mollie Minear¹³⁵, Ryan L. Minster⁴², Braxton D. Mitchell²³, Matt Moll⁶¹, Zeineen Momin³³, May E. Montasser²³, Courtney Montgomery¹³⁶, Donna Muzny³³, Josyf C. Mychaleckyj⁶⁴, Girish Nadkarni⁹⁰, Rakhi Naik²⁶, Take Naseri¹³⁷, Sergei Nekhai¹³⁸, Sarah C. Nelson⁷, Bonnie Neltner⁵⁵, Caitlin Nessner³³, Deborah Nickerson¹³⁰, Osuji Nkechinyere³³, Kari North⁸⁰, Jeff O'Connell²³, Tim O'Connor²³, Heather Ochs-Balcom¹³⁹, Geoffrey Okwuonu³³, Allan Pack¹⁴⁰, David T. Paik¹⁴¹, Nicholette Palmer⁴⁸, James Pankow¹⁴², George Papanicolaou⁴⁰, Cora Parker¹⁴³, Gina Peloso¹⁴⁴, Juan Manuel Peralta⁸¹, Marco Perez³⁰, James Perry²³, Ulrike Peters¹⁴⁵, Patricia Peyser¹⁸, Lawrence S. Phillips²², Jacob Pleiness¹⁸, Toni Pollin²³, Wendy Post¹⁴⁶, Julia Powers Becker¹⁴⁷, Meher Preethi Boorgula⁵⁵, Michael Preuss⁹⁰, Bruce Psaty¹², Pankaj Qasba⁴⁰, Dandi Qiao⁵⁶, Zhaohui Qin²², Nicholas Rafaels¹⁴⁸, Laura Raffield¹⁴⁹, Mahitha Rajendran³³, Vasana S. Ramachandran¹²⁵, D. C. Rao⁸⁸, Laura Rasmussen-Torvik¹⁵⁰, Aakrosh Ratan⁶⁴, Susan Redline⁶¹, Robert Reed²³, Catherine Reeves¹⁷, Elizabeth Regan⁴⁹, Alex Reiner¹⁵¹, Muagututiã Sefuiva Reupena¹⁵², Ken Rice¹², Rebecca Robillard¹⁵³, Nicolas Robine¹⁷, Dan Roden¹⁵⁴, Carolina Roselli¹⁹, Ingo Ruczinski²⁶, Alexi Runnels¹⁷, Pamela Russell⁵⁵, Sarah Ruuska¹⁰⁵, Ester Cerdeira Sabino¹⁵⁵, Danish Saleheen¹⁵⁶, Shabnam Salimi¹⁵⁷, Sejal Salvi³³, Steven Salzberg²⁶, Kevin Sandow¹⁵⁸, Vijay G. Sankaran¹⁵⁹, Jireh Santibanez³³, Karen Schwander⁸⁸, David Schwartz⁵⁵, Frank Sciurba⁴², Christine Seidman¹⁶⁰, Jonathan Seidman¹⁶¹, Frédéric SÃ©ric¹⁶², Vivien Sheehan¹⁶³, Stephanie L. Sherman¹⁶⁴, Amol Shetty²³, Aniket Shetty⁵⁵, Wayne Hui-Heng Sheu¹⁰⁶, M. Benjamin Shoemaker¹⁶⁵, Brian Silver¹⁶⁶, Edwin Silverman⁵⁶, Robert Skomro¹⁶⁷, Albert Vernon Smith¹⁸, Jennifer Smith¹⁸, Josh Smith¹², Nicholas Smith⁹⁹, Tanja Smith¹⁷, Sylvia Smoller¹¹⁰, Beverly Snively¹⁶⁸, Michael Snyder³⁰, Tamar Sofer⁵⁶, Nona Sotoodehnia¹², Adrienne M. Stilp¹², Garrett Storm¹⁶⁹, Elizabeth Streeten²³, Jessica Lasky Su¹⁷⁰, Yun Ju Sung⁸⁸, Jody Sylvia⁵⁶, Adam Szpiro¹², Daniel Taliun¹⁸, Hua Tang¹⁷¹, Margaret Taub²⁶, Matthew Taylor⁹³, Simeon Taylor²³, Marilyn Telen²⁸, Timothy A. Thornton¹², Machiko Threlkeld¹³⁰, Lesley Tinker¹⁷², David Tirschwell¹², Sarah Tishkoff¹⁷³, Hemant Tiwari¹⁷⁴, Catherine Tong⁷, Michael Tsai¹⁴², Dhananjay Vaidya²⁶, David Van Den Berg¹⁷⁵, Peter VandeHaar¹⁸, Scott Vrieze¹⁴², Tarik Walker⁵⁵, Robert Wallace¹⁰², Avram Walts⁵⁵, Fei Fei Wang¹², Heming Wang¹⁷⁶, Jiongming Wang¹⁸, Karol Watson⁶⁰, Jennifer Watt³³, Daniel E. Weeks¹⁷⁷, Joshua Weinstock¹⁰⁹, Bruce Weir¹², Scott T. Weiss¹⁷⁸, Lu-Chen Weng⁸⁵, Jennifer Wessel¹⁷⁹, Cristen Willer⁷¹, Kayleen Williams⁷, L. Keoki Williams¹⁸⁰, Carla Wilson⁵⁶, Lara Winterkorn¹⁷, Quenna Wong¹², Joseph Wu¹⁴¹, Huichun Xu²³, Lisa Yanek²⁶, Ivana Yang⁵⁵, Ketian Yu¹⁸, Seyedeh Maryam Zekavat¹⁹, Yingze Zhang¹⁸¹, Snow Xueyan Zhao⁴⁹, Wei Zhao¹⁸², Xiaofeng Zhu¹⁸³, Elad Ziv¹⁸⁴, Michael Zody¹⁷ & Sebastian Zoellner¹⁸

¹⁷New York Genome Center, New York, New York 10013, US. ¹⁸University of Michigan, Ann Arbor, Michigan 48109, US. ¹⁹Broad Institute, Cambridge, Massachusetts 2142, US. ²⁰Cedars Sinai, Boston, Massachusetts 2114, US. ²¹Children's Hospital of Philadelphia, University of Pennsylvania, Philadelphia, Pennsylvania 19104, US. ²²Emory University, Atlanta, Georgia 30322, US. ²³University of Maryland, Baltimore, Maryland 21201, US. ²⁴University of Mississippi, Jackson, Mississippi 38677, US. ²⁵National Institutes of Health, Bethesda, Maryland 20892, US. ²⁶Johns Hopkins University, Baltimore, Maryland 21218, US. ²⁷University of Kentucky, Lexington, Kentucky 40506, US. ²⁸Duke University, Durham, North Carolina 27708, US. ²⁹University of Alabama, Birmingham, Alabama 35487, US. ³⁰Stanford University, Stanford, California 94305, US. ³¹Medical College of Wisconsin, Milwaukee, Wisconsin 53211, US. ³²Providence Health Care, Medicine, Vancouver, CA, US. ³³Baylor College of Medicine Human Genome Sequencing Center, Houston, Texas 77030, US. ³⁴Cleveland Clinic, Cleveland, Ohio 44195, US. ³⁵Tempus, University of Colorado Anschutz Medical Campus, Aurora, Colorado 80045, US. ³⁶Columbia University, New York, New York 10032, US. ³⁷The Emmes Corporation, LTRC, Rockville, Maryland 20850, US. ³⁸Cleveland Clinic, Quantitative Health Sciences, Cleveland, Ohio 44195, US. ³⁹Johns Hopkins University, Medicine, Baltimore, Maryland 21218, US. ⁴⁰National Heart, Lung, and Blood Institute, National Institutes of Health, Bethesda, Maryland 20892, US. ⁴¹Boston University, Massachusetts General Hospital, Boston University School of Medicine, Boston, Massachusetts 2114, US. ⁴²University of Pittsburgh, Pittsburgh, Pennsylvania 15260, US. ⁴³FundaÃ§Ã£o de Hematologia e Hemoterapia de Pernambuco - Hemope, Recife 52011-000 BR,

Brazil. ⁴⁴University of Washington, Cardiovascular Health Research Unit, Department of Medicine, Seattle, Washington 98195, US. ⁴⁵University of Texas Rio Grande Valley School of Medicine, Human Genetics, Brownsville, Texas 78520, US. ⁴⁶University of Utah, Obstetrics and Gynecology, Salt Lake City, Utah 84132, US. ⁴⁷University of Texas Health at Houston, Houston, Texas 77225, US. ⁴⁸Wake Forest Baptist Health, Department of Biochemistry, Winston-Salem, North Carolina 27157, US. ⁴⁹National Jewish Health, National Jewish Health, Denver, Colorado 80206, US. ⁵⁰Medical College of Wisconsin, Pediatrics, Milwaukee, Wisconsin 53226, US. ⁵¹University of Texas Health at Houston, Pediatrics, Houston, Texas 77030, US. ⁵²University of California, San Francisco, San Francisco, California 94143, US. ⁵³Stanford University, Biomedical Data Science, Stanford, California 94305, US. ⁵⁴Brigham & Women's Hospital, Brigham and Women's Hospital, Boston, Massachusetts 2115, US. ⁵⁵University of Colorado at Denver, Denver, Colorado 80204, US. ⁵⁶Brigham & Women's Hospital, Boston, Massachusetts 2115, US. ⁵⁷University of Montreal, US, Montreal, Canada. ⁵⁸University of Mississippi, Medicine, Jackson, Mississippi 39213, US. ⁵⁹Washington State University, Pullman, Washington 99164, US. ⁶⁰University of California, Los Angeles, Los Angeles, California 90095, US. ⁶¹Brigham & Women's Hospital, Medicine, Boston, Massachusetts 2115, US. ⁶²National Taiwan University, Taipei 10617 TW, China. ⁶³Brigham & Women's Hospital, Division of Preventive Medicine, Boston, Massachusetts 2215, US. ⁶⁴University of Virginia, Charlottesville, Virginia 22903, US. ⁶⁵National Taiwan University, National Taiwan University Hospital, Taipei 10617 TW, China. ⁶⁶National Health Research Institute Taiwan, Miaoli County 350 TW, China. ⁶⁷Cleveland Clinic, Immunity and Immunology, Cleveland, Ohio 44195, US. ⁶⁸University of Vermont, Burlington, Vermont 5405, US. ⁶⁹Boston University, Biostatistics, Boston, Massachusetts 2115, US. ⁷⁰University of Texas Rio Grande Valley School of Medicine, Brownsville, Texas 78520, US. ⁷¹University of Michigan, Internal Medicine, Ann Arbor, Michigan 48109, US. ⁷²Vitalant Research Institute, San Francisco, California 94118, US. ⁷³University of Illinois at Chicago, Chicago, Illinois 60607, US. ⁷⁴University of Chicago, Chicago, Illinois 60637, US. ⁷⁵Mayo Clinic, Health Quantitative Sciences Research, Rochester, Minnesota 55905, US. ⁷⁶Washington University in St Louis, Department of Medicine, Cardiovascular Division, St. Louis, Missouri 63110, US. ⁷⁷University of Texas Health at Houston, Human Genetics Center, Department of Epidemiology, Human Genetics, and Environmental Sciences, Houston, Texas 77030, US. ⁷⁸Vanderbilt University, Nashville, Tennessee 37235, US. ⁷⁹University of Cincinnati, Cincinnati, Ohio 45220, US. ⁸⁰University of North Carolina, Chapel Hill, North Carolina 27599, US. ⁸¹University of Texas Rio Grande Valley School of Medicine, Edinburg, Texas 78539, US. ⁸²Washington University in St Louis, Genetics, St Louis, Missouri 63110, US. ⁸³Brown University, Providence, Rhode Island 2912, US. ⁸⁴Harvard University, Channing Division of Network Medicine, Cambridge, Massachusetts 2138, US. ⁸⁵Massachusetts General Hospital, Boston, Massachusetts 2114, US. ⁸⁶National Jewish Health, Center for Genes, Environment and Health, Denver, Colorado 80206, US. ⁸⁷University of North Carolina, Epidemiology, Chapel Hill, North Carolina 27599, US. ⁸⁸Washington University in St Louis, St Louis, Missouri 63130, US. ⁸⁹Fred Hutchinson Cancer Research Center, Seattle, Washington 98109, US. ⁹⁰Icahn School of Medicine at Mount Sinai, New York, New York 10029, US. ⁹¹Boston Children's Hospital, Harvard Medical School, Department of Psychiatry, Boston, Massachusetts 2115, US. ⁹²University of Texas Rio Grande Valley School of Medicine, San Antonio, Texas 78229, US. ⁹³University of Colorado Anschutz Medical Campus, Aurora, Colorado 80045, US. ⁹⁴Mass General Brigham, Obstetrics and Gynecology, Boston, Massachusetts 2115, US. ⁹⁵University of Calgary, Medicine, Calgary, CA, Canada. ⁹⁶University of Maryland, Genetics, Philadelphia, Pennsylvania 19104, US. ⁹⁷Yale University, Department of Chronic Disease Epidemiology, New Haven, Connecticut 6520, US. ⁹⁸Tulane University, New Orleans, Louisiana 70118, US. ⁹⁹University of Washington, Epidemiology, Seattle, Washington 98195, US. ¹⁰⁰Wake Forest Baptist Health, Winston-Salem, North Carolina 27157, US. ¹⁰¹Brigham & Women's Hospital, Channing Division of Network Medicine, Boston, Massachusetts 2115, US. ¹⁰²University of Iowa, Iowa City, Iowa 52242, US. ¹⁰³National Health Research Institute Taiwan, Institute of Population Health Sciences, NHRI, Miaoli County 350 TW, China. ¹⁰⁴Tri-Service General Hospital National Defense Medical Center, Taipei, TW, China. ¹⁰⁵Blood Works Northwest, Seattle, Washington 98104, US. ¹⁰⁶Taichung Veterans General Hospital Taiwan, Taichung City 407 TW, China. ¹⁰⁷Oklahoma State University Medical Center, Internal Medicine, Division of Endocrinology, Diabetes and Metabolism, Columbus, Ohio 43210, US. ¹⁰⁸Blood Works Northwest, Research Institute, Seattle, Washington 98104, US. ¹⁰⁹University of Michigan, Biostatistics, Ann Arbor, Michigan 48109, US. ¹¹⁰Albert Einstein College of Medicine, New York, New York 10461, US. ¹¹¹University of California, San Francisco, San Francisco, California 94118, US. ¹¹²Harvard University, Cambridge, Massachusetts 2138, US. ¹¹³McGill University, Montréal, QC, H3A 0G4 Montreal, CA, Canada. ¹¹⁴University of Colorado at Denver, Epidemiology, Aurora, Colorado 80045, US. ¹¹⁵Blood Works Northwest, Medicine, Seattle, Washington 98104, US. ¹¹⁶Loyola University, Public Health Sciences, Maywood, Illinois 60153, US. ¹¹⁷Harvard School of Public Health, Biostats, Boston, Massachusetts 2115, US. ¹¹⁸University of Colorado at Denver, Medicine, Aurora, Colorado 80048, US. ¹¹⁹Lundquist Institute, Torrance, California 90502, US. ¹²⁰Boston University, University of Massachusetts Chan Medical School, Worcester, Massachusetts 1655, US. ¹²¹Harvard School of Public Health, Boston, Massachusetts 2115, US. ¹²²Brown University, Epidemiology and Medicine, Providence, Rhode Island 2912, US. ¹²³Stanford University, Cardiovascular Institute, Stanford, California 94305, US. ¹²⁴Icahn School of Medicine at Mount Sinai, The Charles Bronfman Institute for Personalized Medicine, New York, New York 10029, US. ¹²⁵Boston University, Boston, Massachusetts 2215, US. ¹²⁶Ohio State University, Division of Pulmonary, Critical Care and Sleep Medicine, Columbus, Ohio 43210, US. ¹²⁷Broad Institute, Harvard University, Massachusetts General Hospital, Boston, US. ¹²⁸George Washington University, cardiology, Washington, District of Columbia 20037, US. ¹²⁹Brown University, Epidemiology, Providence, Rhode Island 2912, US. ¹³⁰University of Washington, Department of Genome Sciences, Seattle, Washington 98195, US. ¹³¹RTI International, Boston, US. ¹³²Massachusetts General Hospital, Medicine, Boston, Massachusetts 2114, US. ¹³³University of Arizona, Tucson, Arizona 85721, US. ¹³⁴Stanford University, Center For Sleep Sciences and Medicine, Palo Alto, California 94304, US. ¹³⁵National Institute of Child Health and Human Development, National Institutes of Health, Bethesda, Maryland 20892, US. ¹³⁶Oklahoma Medical Research Foundation, Genes and Human Disease, Oklahoma City, Oklahoma 73104, US. ¹³⁷Ministry of Health, Government of Samoa, Apia, WS, Samoa. ¹³⁸Howard University, Washington, District of Columbia 20059, US. ¹³⁹University at Buffalo, Buffalo, New York 14260, US. ¹⁴⁰University of Pennsylvania, Division of Sleep Medicine/Department of Medicine, Philadelphia, Pennsylvania 19104-3403, US. ¹⁴¹Stanford University, Stanford Cardiovascular Institute, Stanford, California 94305, US. ¹⁴²University of Minnesota, Minneapolis, Minnesota 55455, US. ¹⁴³RTI International, Biostatistics and Epidemiology Division, Research Triangle Park, North Carolina 27709-2194, US. ¹⁴⁴Boston University, Department of Biostatistics, Boston, Massachusetts 2118, US. ¹⁴⁵Fred Hutchinson Cancer Research Center, Fred Hutch and UW, Seattle, Washington 98109, US. ¹⁴⁶Johns Hopkins University, Cardiology/Medicine, Baltimore, Maryland 21218, US. ¹⁴⁷University of Colorado at Denver, Medicine, Denver, Colorado 80204, US. ¹⁴⁸University of Colorado at Denver, CCPM, Denver, Colorado 80045, US. ¹⁴⁹University of North Carolina, Genetics, Chapel Hill, North Carolina 27599, US. ¹⁵⁰Northwestern University, Chicago, Illinois 60208, US. ¹⁵¹Fred Hutchinson Cancer Research Center, University of Washington, Seattle, Washington 98109, US. ¹⁵²Lutia I Puava Ae Mapu I Fagalele, Apia, WS, Samoa. ¹⁵³University of Ottawa, Sleep Research Unit, University of Ottawa Institute for Mental Health Research, Ottawa ON K1Z 7K4 CA, Canada. ¹⁵⁴Vanderbilt University, Medicine, Pharmacology, Biomedical Informatics, Nashville, Tennessee 37235, US. ¹⁵⁵Universidade de Sao Paulo, Faculdade de Medicina, Sao Paulo 1310000 BR, Brazil. ¹⁵⁶Columbia University, New York, New York 10027, US. ¹⁵⁷University of Maryland, Pathology, Seattle, Washington 98195, US. ¹⁵⁸Lundquist Institute, TGPS, Torrance, California 90502, US. ¹⁵⁹Harvard University, Division of Hematology/Oncology, Boston, Massachusetts 2115, US. ¹⁶⁰Harvard Medical School, Genetics, Boston, Massachusetts 2115, US. ¹⁶¹Harvard Medical School, Boston, Massachusetts 2115, US. ¹⁶²Université Laval, Quebec City G1V 0A6 CA, Canada. ¹⁶³Emory University, Pediatrics, Atlanta, Georgia 30307, US. ¹⁶⁴Emory University, Human Genetics, Atlanta, Georgia 30322, US. ¹⁶⁵Vanderbilt University, Medicine/ Cardiology, Nashville, Tennessee 37235, US. ¹⁶⁶UMass Memorial Medical Center, Worcester, Massachusetts 1655, US. ¹⁶⁷University of Saskatchewan, Saskatoon SK S7N 5C9 CA, Canada. ¹⁶⁸Wake Forest Baptist Health, Biostatistical Sciences, Winston-Salem, North Carolina 27157, US. ¹⁶⁹University of Colorado at

Denver, Genomic Cardiology, Aurora, Colorado 80045, US. ¹⁷⁰Brigham & Women's Hospital, Channing Department of Medicine, Boston, Massachusetts 2115, US. ¹⁷¹Stanford University, Genetics, Stanford, California 94305, US. ¹⁷²Fred Hutchinson Cancer Research Center, Cancer Prevention Division of Public Health Sciences, Seattle, Washington 98109, US. ¹⁷³University of Pennsylvania, Genetics, Philadelphia, Pennsylvania 19104, US. ¹⁷⁴University of Alabama, Biostatistics, Birmingham, Alabama 35487, US. ¹⁷⁵University of Southern California, USC Methylation Characterization Center, University of Southern California, California 90033, US. ¹⁷⁶Brigham & Women's Hospital, Mass General Brigham, Boston, Massachusetts 2115, US. ¹⁷⁷University of Pittsburgh, Department of Human Genetics, Pittsburgh, Pennsylvania 15260, US. ¹⁷⁸Brigham & Women's Hospital, Channing Division of Network Medicine, Department of Medicine, Boston, Massachusetts 2115, US. ¹⁷⁹Indiana University, Epidemiology, Indianapolis, Indiana 46202, US. ¹⁸⁰Henry Ford Health System, Detroit, Michigan 48202, US. ¹⁸¹University of Pittsburgh, Medicine, Pittsburgh, Pennsylvania 15260, US. ¹⁸²University of Michigan, Department of Epidemiology, Ann Arbor, Michigan 48109, US. ¹⁸³Case Western Reserve University, Department of Population and Quantitative Health Sciences, Cleveland, Ohio 44106, US. ¹⁸⁴University of California, San Francisco, US.